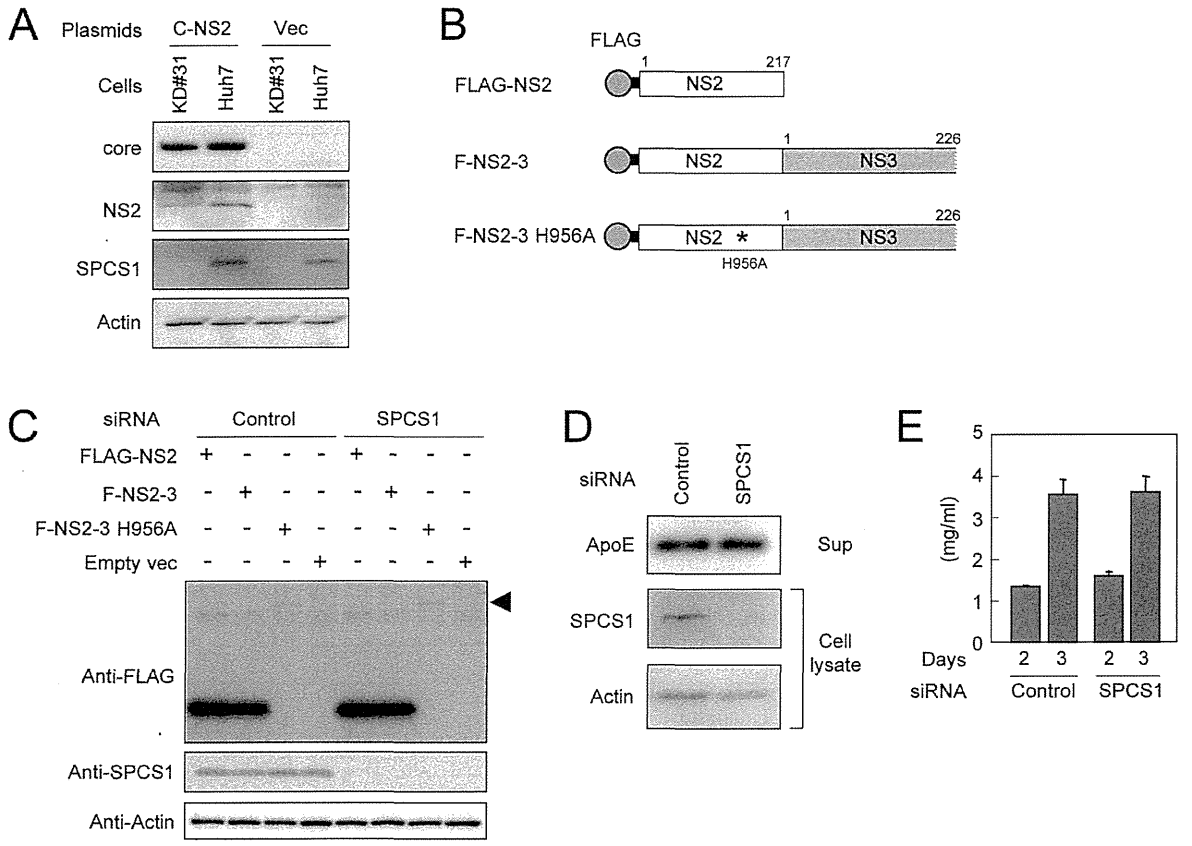

Figure 4. Effect of SPCS1 knockdown on the processing of HCV structural proteins and secretion of host proteins. (A) Core-NS2 polyprotein was expressed in KD#31 cells or parental Huh-7 cells. Core, NS2, SPCS1, and actin were detected by immunoblotting 2 days post-transfection. (B) Expression constructs of NS2 and NS2/3 proteins. His to Ala substitution mutation at aa 956 in NS2 is indicated by an asterisk. Gray circles and bold lines indicate FLAG-tag and the spacer sequences, respectively. Positions of the aa residues are indicated above the boxes. (C) Effect of SPCS1 knockdown on processing at the NS2/3 junction. Huh-7 cells were transfected with SPCS1 siRNA or control siRNA at a final concentration of 30 nM, and then transfected with plasmids for FLAG-NS2, F-NS2-3, or F-NS2-3 with a protease-inactive mutation (H956A). NS2 in cell lysates was detected by anti-FLAG antibody 2 days post-transfection. Arrowhead indicates unprocessed NS2-3 polyproteins. (D) Effect of SPCS1 knockdown on the secretion of apoE. Huh7.5.1 cells were transfected with SPCS1 siRNAs or control siRNA at a final concentration of 20 nM, and apoE in the supernatant and SPCS1 and actin in the cells were detected 3 days post-transfection. (E) Effect of SPCS1 knockdown on the secretion of albumin. Huh7.5.1 cells were transfected with SPCS1 siRNA or control siRNA, and albumin in the culture supernatants at 2 and 3 days post-transfection was measured by ELISA.
doi:10.1371/journal.ppat.1003589.g004

with expression plasmids for E2, FLAG-NS2, and SPCS1-myc. E2 and NS2 were co-immunoprecipitated with SPCS1-myc, and E2 and SPCS1-myc were co-immunoprecipitated with FLAG-NS2 (Fig. 6A), suggesting the formation of an E2-NS2-SPCS1 complex in cells. To investigate the interaction of SPCS1 with E2 in the absence of NS2, HCV Core-p7 polyprotein or E2 protein were co-expressed with SPCS1-myc in cells, followed by immunoprecipitation with anti-myc antibody. As shown in Fig. 6B and Fig. S2, E2 was co-immunoprecipitated with SPCS1-myc. The interaction between SPCS1 and E2 was further analyzed *in situ* by PLA and mKG system. Specific signals indicating formation of the SPCS1-E2 complex were detected in both assays (Fig. S3), suggesting physical interaction between SPCS1 and E2 in cells.

We further determined the region of SPCS1 responsible for the interaction with E2 by co-immunoprecipitation assays. Full-length and deletion mutant d2 of SPCS1 (Fig. 1A) were similarly co-immunoprecipitated with E2, while only a limited amount of d1 mutant SPCS1 (Fig. 1A) was co-precipitated (Fig. 6C). It may be that the aa 43–102 region of SPCS1, which was identified as the region involved in the NS2 interaction (Fig. 1D), is important for its interaction with E2, and that deletion of the N-terminal cytoplasmic region leads to misfolding of the protein and subsequent inaccessibility to E2.

Finally, to understand the significance of SPCS1 in the NS2-E2 interaction, Huh7.5.1 cells with or without SPCS1 knockdown by siRNA were transfected with expression plasmids for Core-p7 and FLAG-NS2, followed by co-immunoprecipitation with anti-FLAG antibody. As shown in Fig. 6D, the NS2-E2 interaction was considerably impaired in the SPCS1-knockdown cells as compared to that in the control cells. A similar result was obtained in the stable SPCS1-knockdown cell line (Fig. 6E). In contrast, in that cell line, the interaction of NS2 with NS3 was not impaired by SPCS1 knockdown (Fig. 6E).

These results, together with the above findings, suggest that SPCS1 is required for or facilitates the formation of the membrane-associated NS2-E2 complex, which participates in the proper assembly of infectious particles.

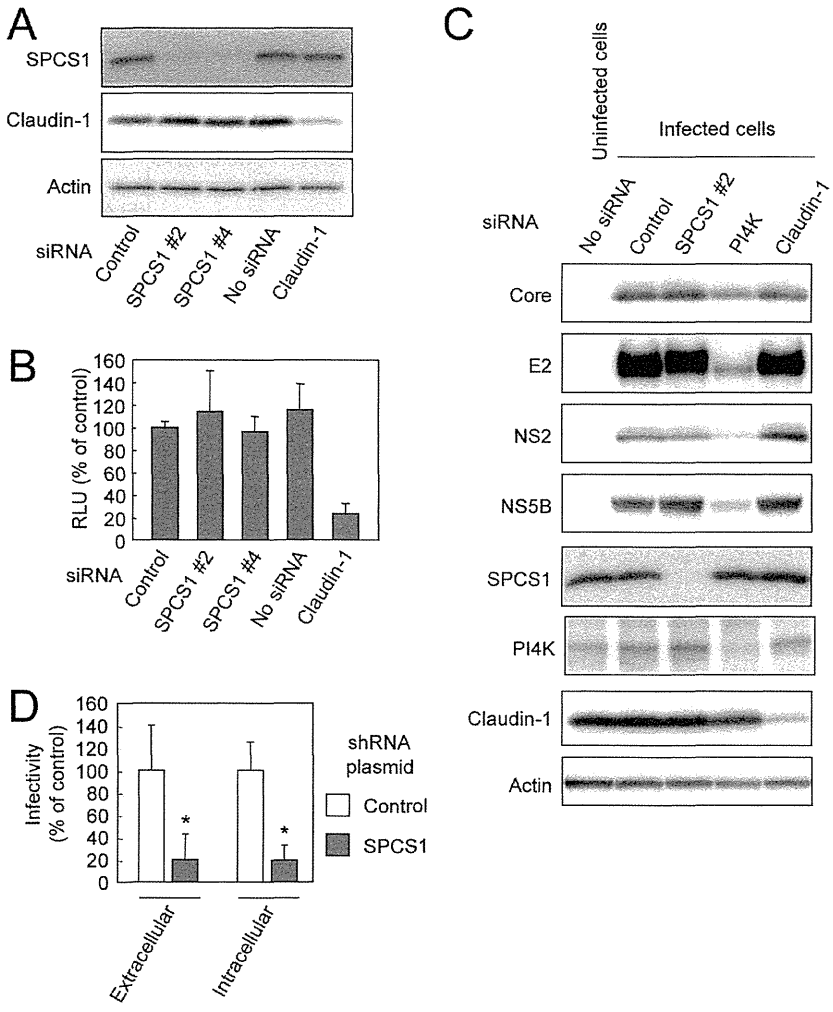

Figure 5. Effect of SPCS1 knockdown on entry into cells, genome replication, and assembly or release of infectious virus. (A) Huh7.5.1 cells were transfected with siRNA for SPCS1 or claudin1, or control siRNA at a final concentration of 30 nM. Expression levels of endogenous SPCS1, claudin-1, and actin in the cells at 2 days post-transfection were examined by immunoblotting using anti-SPCS1, anti-actin, and anti-claudin-1 antibodies. (B) Huh7.5.1 cells transfected with indicated siRNAs were infected with HCVtcp at 2 days post-transfection. Luciferase activity in the cells was subsequently determined at 2 days post-infection. Data are averages of triplicate values with error bars showing standard deviations. (C) Effect of SPCS1 knockdown on replication of HCV genome. HCV-infected Huh-7 cells transfected with siRNA for SPCS1, PI4K or claudin1, or control siRNA at a final concentration of 30 nM. Expression levels of HCV proteins as well as endogenous SPCS1, PI4K, claudin-1, and actin in the cells at 3 days post-transfection were examined by immunoblotting. (D) HCV infectivity in Huh7.5.1 cells inoculated with culture supernatant and cell lysate from Huh7-25 cells transfected with pSilencer-SPCS1 or control vector along with pHH/JFH1am at 5 days post-transfection. Statistical differences between Control and SPCS1 knockdown were evaluated using Student's t-test. *$p<0.005$ vs. Control.
doi:10.1371/journal.ppat.1003589.g005

Discussion

In this study, we identified SPCS1 as a novel host factor that interacts with HCV NS2, and showed that SPCS1 participates in HCV assembly through complex formation with NS2 and E2. In general, viruses require host cell-derived factors for proceeding and regulating each step in their lifecycle. Although a number of host factors involved in genome replication and cell entry of HCV have been reported, only a few for viral assembly have been identified to date. To our knowledge, this is the first study to identify an NS2-interacting host protein that plays a role in the production of infectious HCV particles.

NS2 is a hydrophobic protein containing TM segments in the N-terminal region. The C-terminal half of NS2 and the N-terminal third of NS3 form the protease, which is a prerequisite for NS2-NS3 cleavage. In addition, it is now accepted that this protein is essential for particle production [4–6,12]. However, the mechanism of how NS2 is involved in the assembly process of HCV has been unclear.

So far, two studies have screened for HCV NS2 binding proteins by yeast two-hybrid analysis [37,38]. Erdtmann et al. reported that no specific interaction was detected by a conventional yeast hybrid screening system using full-length NS2 as a bait, probably due to hampered translocation of the bait to the

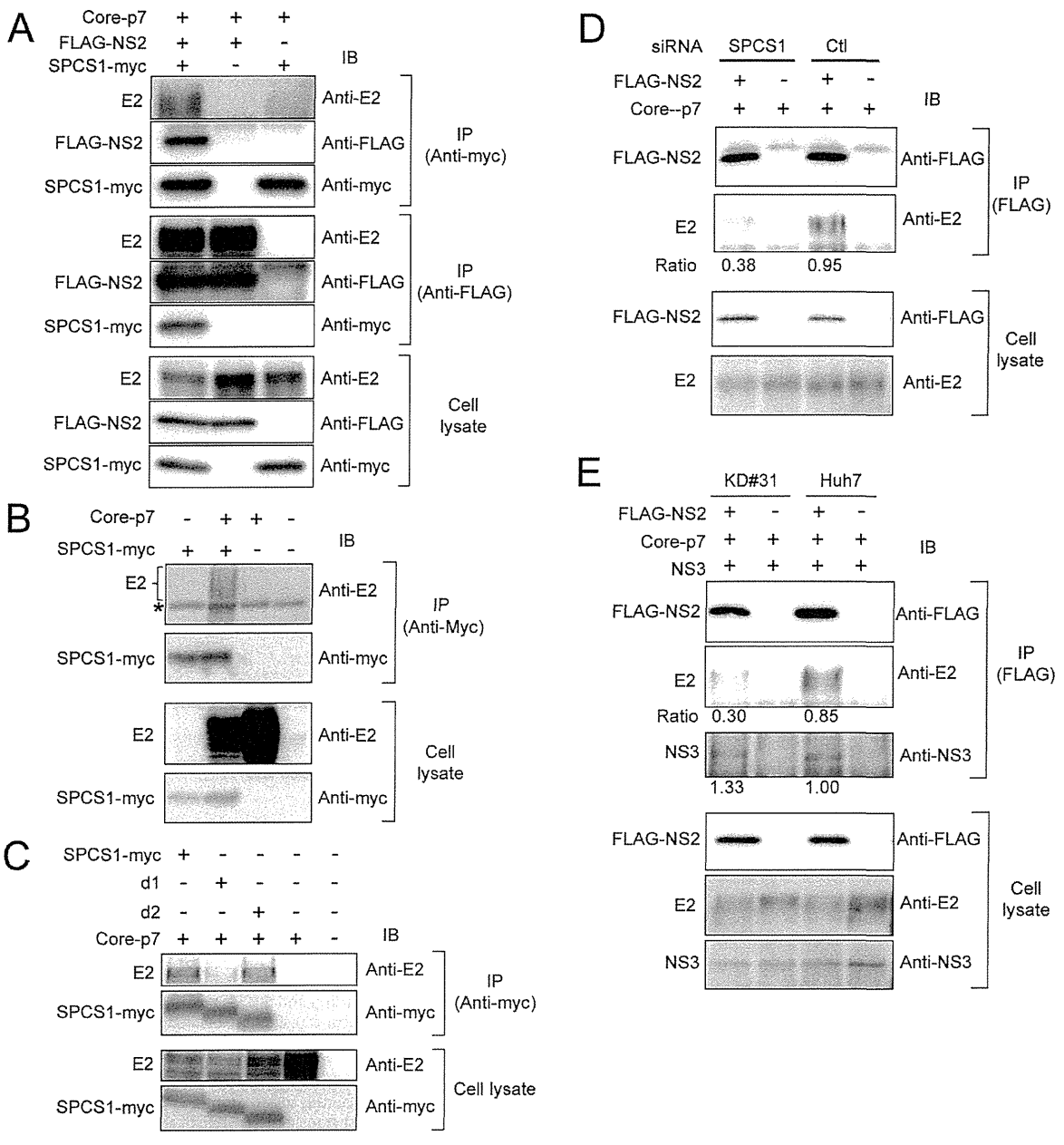

Figure 6. SPCS1 forms a complex with NS2 and E2. (A) Lysates of cells, which were co-transfected with Core-p7, FLAG-NS2, and SPCS1-myc expression plasmids, were immunoprecipitated with anti-myc or anti-FLAG antibody. The resulting precipitates and whole cell lysates used in IP were examined by immunoblotting using anti-E2, anti-FLAG, or anti-myc antibody. An empty plasmid was used as a negative control. (B) Cells were transfected with Core-p7 expression plasmid in the presence or absence of SPCS1-myc expression plasmid. The cell lysates of the transfected cells were immunoprecipitated with anti-myc antibody. The resulting precipitates and whole cell lysates used in IP were examined by immunoblotting using anti-E2 or anti-myc antibody. An empty plasmid was used as a negative control. The bands corresponding to immunoglobulin heavy chain are marked by an asterisk. (C) Cells were co-transfected with Core-p7 and SPCS1-myc expression plasmids. The cell lysates of the transfected cells were immunoprecipitated with anti-myc antibody. The resulting precipitates and whole cell lysates used in IP were examined by immunoblotting using anti-E2 or anti-myc antibody. (D) Huh7.5.1 cells were transfected with SPCS1 siRNA or control siRNA at a final concentration of 20 nM. After 24 h, Huh7.5.1 cells were then co-transfected with FLAG-NS2 and Core-p7 expression plasmids. The lysates of transfected cells were immunoprecipitated with anti-FLAG antibody, followed by immunoblotting with anti-FLAG and anti-E2 antibodies. Immunoblot analysis of whole cell lysates was also performed. Intensity of E2 bands was quantified, and the ratio of immunoprecipitated E2 to E2 in cell lysate was shown. Similar results were obtained in 2 independent experiments. (E) KD#31 cells and parental Huh-7 cells were co-transfected with FLAG-NS2, Core-p7, and NS3 expression plasmids. The lysates of transfected cells were immunoprecipitated with anti-FLAG antibody followed by immunoblotting with anti-FLAG, anti-E2, and anti-NS3 antibodies. Immunoblot analysis of whole cell lysates was also performed. The ratio of immunoprecipitated E2 or NS3 to E2 or NS3 in cell lysate, respectively, were shown.

doi:10.1371/journal.ppat.1003589.g006

nucleus [37]. They further screened a human liver cDNA library using NS2 with deletion of the N-terminal TM domain, and CIDE-B protein, a member of the CIDE family of apoptosis-inducing factors, was identified. However, whether CIDE-B is involved in the HCV lifecycle and/or viral pathogenesis is unclear. de Chassey et al. reported several cellular proteins as potential NS2 binding proteins using NS2 with N-terminal deletion as a bait [38]. Involvement of these proteins in the HCV lifecycle is also unclear. In our study, to screen for NS2-binding partners using full-length NS2 as a bait, we utilized a split-ubiquitin yeast two-hybrid system that allows for the identification of interactions between full-length integral membrane proteins or between a full-length membrane-associated protein and a soluble protein [39]. SPCS1 was identified as a positive clone of an NS2-binding protein, but proteins that have been reported to interact with NS2 were not selected from our screening.

SPCS1 is a component of the signal peptidase complex that processes membrane-associated and secreted proteins in cells. The mammalian signal peptidase complex consists of five subunits, SPCS1, SPCS2, SPCS3, SEC11A, and SEC11C [27]. Among them, the functional role of SPCS1 is still unclear, and SPCS1 is considered unlikely to function as a catalytic subunit according to membrane topology [40]. The yeast homolog of SPCS1, Spc1p, is also known to be nonessential for cell growth and enzyme activity [28,41]. Interestingly, these findings are consistent with the results obtained in this study. Knockdown of SPCS1 did not impair processing of HCV structural proteins (Fig. 4A) or secretion of apoE and albumin (Fig. 4B and C), which are regulated by ER membrane-associated signal peptidase activity. The propagation of JEV, whose structural protein regions are cleaved by signal peptidase, was also not affected by the knockdown of SPCS1 (Fig. 3B). SPCS1, SPCS2, and SPCS3 are among the host factors that function in HCV production identified from genome-wide siRNA screening [42]. It seemed that knockdown of SPCS1 had a higher impact on the later stage of viral infection compared to either SPCS2 or SPCS3, which are possibly involved in the catalytic activity of the signal peptidase.

Further analyses to address the mechanistic implication of SPCS1 on the HCV lifecycle revealed that SPCS1 knockdown impaired the assembly of infectious viruses in the cells, but not cell entry, RNA replication, or release from the cells (Fig. 5). We thus considered the possibility that the SPCS1-NS2 interaction is important for the role of NS2 in viral assembly. Several studies have reported that HCV NS2 is associated biochemically or genetically with viral structural proteins as well as NS proteins [10,18–25]. As an intriguing model, it has been proposed that NS2 functions as a key organizer of HCV assembly and plays a key role in recruiting viral envelope proteins and NS protein(s) such as NS3 to the assembly sites in close proximity to lipid droplets [21]. The interaction of NS2 with E2 has been shown by use of an HCV genome encoding tagged-NS2 protein in virion-producing cells. Furthermore, the selection of an assembly-deficient NS2 mutation located within its TM3 for pseudoreversion leads to a rescue mutation in the TM domain of E2, suggesting an in-membrane interaction between NS2 and E2 [21]. Another study identified two classes of NS2 mutations with defects in virus assembly; one class leads to reduced interaction with NS3, and the other, located in the TM3 domain, maintains its interaction with NS3 but shows impaired interaction between NS2 and E1-E2 [20]. However, the precise details of the NS2-E2 interaction, such as direct protein-protein binding or participating host factors, are unknown. Our results provide evidence that SPCS1 has an important role in the formation of the NS2-E2 complex by its interaction with both NS2 and E2, most likely via their transmembrane domains, including TM3 of NS2. As knockdown of SPCS1 reduced the interaction of NS2 and E2 as shown in Fig. 6D and E, it may be that SPCS1 contributes to NS2-E2 complex formation or to stabilizing the complex. Based on data obtained in this study, we propose a model of the formation of an E2-SPCS1-NS2 complex at the ER membrane (Fig. 7).

In summary, we identified SPCS1 as a novel NS2-binding host factor required for HCV assembly by split-ubiquitin membrane yeast two-hybrid screening. Our data demonstrate that SPCS1 plays a key role in the E2-NS2 interaction via formation of an E2-SPCS1-NS2 complex. These findings provide clues for understanding the molecular mechanism of assembly and formation of infectious HCV particles.

Materials and Methods

Split ubiquitin-based yeast two-hybrid screen

A split-ubiquitin membrane yeast two-hybrid screen was performed to identify possible NS2 binding partners. This screening system (DUALmembrane system; Dualsystems Biotech, Schlieren, Switzerland) is based on an adaptation of the ubiquitin-based split protein sensor [26]. The full-length HCV NS2 gene derived from the JFH-1 strain [29] was cloned into pBT3-SUC bait vector to obtain bait protein fused to the C-terminal half of ubiquitin (NS2-Cub) along with a transcription factor. Prey proteins generated from a human liver cDNA library (Dualsystems Biotech) were expressed as a fusion to the N-terminal half of ubiquitin (NubG). Complex formation between NS2-Cub and NubG-protein from the library leads to cleavage at the C-terminus of reconstituted ubiquitin by ubiquitin-specific protease(s) and consequent translocation of the transcription factor into the nucleus. Library plasmids were recovered from positive transformants, followed by determining the nucleotide sequences of inserted cDNAs, which were identified using the BLAST algorithm with the GenBank database.

Cell culture

Human embryonic kidney 293T cells, and human hepatoma Huh-7 cells and its derivative cell lines Huh7.5.1 [43] and Huh7-25 [36], were maintained in Dulbecco's modified Eagle medium supplemented with nonessential amino acids, 100 U of penicillin/ml, 100 μg of streptomycin/ml, and 10% fetal bovine serum (FBS) at 37°C in a 5% CO_2 incubator.

Plasmids

Plasmids pCAGC-NS2/JFH1am and pHHJFH1am were previously described [33]. The plasmid pCAGC-p7/JFHam, having

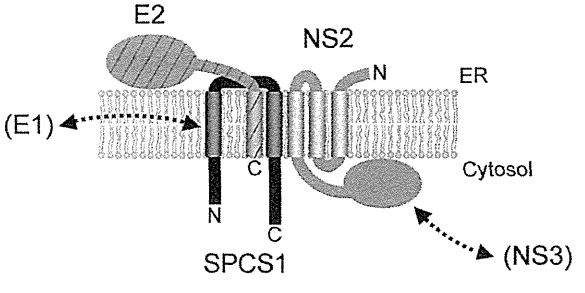

Figure 7. A proposed model for a complex consisting of NS2, SPCS1 and E2 associated with ER membranes.
doi:10.1371/journal.ppat.1003589.g007

adaptive mutations in E2 (N417S) and p7 (N765D) in pCAG/C-p7 [44], was constructed by oligonucleotide-directed mutagenesis.

To generate the NS2 expression plasmid pCAG F-NS2 and the NS2-deletion mutants, cDNAs encoding the full-length or parts of NS2 possessing the FLAG-tag and spacer sequences (MDYKDDDDKGGGGS) were amplified from pCAGC-NS2/JFH1am by PCR. The resultant fragments were cloned into pCAGGS. For the NS2-NS3 expression plasmid pEF F-NS2-3, a cDNA encoding the entire NS2 and the N-terminal 226 amino acids of NS3 with the N-terminal FLAG-tag sequence as above was amplified by PCR and was inserted into pEF1/myc-His (Invitrogen, Carlsbad, CA). The plasmid pEF F-NS2-3 H956A, having a defective mutation in the protease active site within NS2, was constructed by oligonucleotide-directed mutagenesis.

To generate the NS3 expression plasmid pCAGN-HANS3JFH1, a cDNA encoding NS3 with an HA tag at the N terminus, which was amplified by PCR with pHHJFHam as a template, was inserted downstream of the CAG promoter of pCAGGS.

To generate the SPCS1-expressing plasmid pCAG-SPCS1-myc and its deletion mutants, cDNAs encoding all of or parts of SPCS1 with the Myc tag sequence (EQKLISEEDL) at the C-terminus, which was amplified by PCR, was inserted into pCAGGS. pSilencer-shSPCS1 carrying a shRNA targeted to SPCS1 under the control of the U6 promoter was constructed by cloning the oligonucleotide pair 5′- GATCCGCAATAGTTGGATTTATCT TTCAAGAGAAGATAAATCCAACTATTGCTTTTTTGGA AA-3′ and 5′- AGCTTTTCCAAAAAAGCAATAGTTGGATT-TATCTTCTCTTGAAAGATAAATCCAACTATTGCG-3′ between the BamHI and HindIII sites of pSilencer 2.1-U6 hygro (Ambion, Austin, TX). To generate a construct expressing shRNA-resistant SPCS1 pSPCS1-sh^r, a cDNA fragment coding for SPCS1, in which the 6 bp within the shRNA targeting region (5′-GCAATAGTTGGATTTATCT-3′) was replaced with GCT ATTGTCGGCTTCATAT that causes no aa change, was amplified by PCR. The resulting fragment was confirmed by sequencing and then cloned into pCAGGS.

Full-length SPCS1 and N-terminal region of NS2 (aa 1–94) were amplified by PCR and cloned onto EcoRI and HindIII sites of phmKGN-MN and phmKGC-MN, which encode the mKG fragments (CoralHue Fluo-chase Kit; MBL, Nagoya, Japan), designated as pSPCS1-mKG(N) and pNS2-mKG(C), respectively. Transmembrane domain of the E1 to E2 was also amplified by PCR and cloned onto EcoRI and HindIII sites of phmKGC-MN. To avoid the cleavage of E2-mKG(C) fusion protein in the cells, last alanine of the E2 protein was deleted. Positive control plasmids for mKG system, pCONT-1 and pCONT-2, which encode p65 partial domain from NF-κB complex fused to mKG(N) and p50 partial domain from NF-κB complex fused to mKG(C) respectively, were supplied from MBL. For PLA experiments, cDNA for SPCS1 d2-myc with the V5 tag at the N-terminus was amplified by PCR, and inserted into pCAGGS. For expression of HCV E2, cDNA from E1 signal to the last codon of the transmembrane domain of the E2, in which part of the hypervariable region-1 (aa 394–400) were replaced with FLAG-tag and spacer sequences (DYKDDDDKGGG), was amplified by PCR, and inserted into pCAGGS. For expression of FLAG-core, cDNAs encoding Core (aa 1–152) possessing the FLAG-tag and spacer sequences (MDYKDDDDKGGGGS) were amplified from pCAGC191 [45] by PCR. The resultant fragments were cloned into pCAGGS.

DNA transfection

Monolayers of 293T cells were transfected with plasmid DNA using FuGENE 6 transfection reagent (Roche, Basel, Switzerland) in accordance with the manufacturer's instructions. Huh-7, Huh7.5.1, and Huh7-25 cells were transfected with plasmid DNA using TransIT LT1 transfection reagent (Mirus, Madison, WI).

PLA

The assay was performed in a humid chamber at 37°C according to the manufacturer's instructions (Olink Bioscience, Uppsala, Sweden). Transfected 293T cells were grown on glass coverslips. Two days after transfection, cells were fixed with 4% paraformaldehyde in phosphate-buffered saline (PBS) for 20 min, then blocked and permeabilized with 0.3% Triton X-100 in a nonfat milk solution (Block Ace; Snow Brand Milk Products Co., Sapporo, Japan) for 60 min at room temperature. Then the samples were incubated with a mixture of mouse anti-FLAG monoclonal antibody M2 and rabbit anti-V5 polyclonal antibody for 60 min, washed three times, and incubated with plus and minus PLA probes. After washing, the ligation mixture containing connector oligonucleotide was added for 30 min. The washing step was repeated, and amplification mixture containing fluorescently labeled DNA probe was added for 100 min. Finally, the samples were washed and mounted with DAPI mounting medium. The signal representing interaction was analyzed by Leica TCS SPE confocal microscope.

mKG system

The assay was performed according to the manufacturer's instructions (CoralHue Fluo-chase Kit; MBL). 293T cells were transfected by a pair of mKG fusion constructs. Twenty-four hours after transfection, cell were fixed and stained with DAPI. The signal representing interaction was analyzed by Leica TCS SPE confocal microscope.

Gene silencing by siRNA

The siRNAs were purchased from Sigma-Aldrich (St. Louis, MO) and were introduced into the cells at a final concentration of 10 to 30 nM using Lipofectamine RNAiMAX (Invitrogen). Target sequences of the siRNAs were as follows: SPCS1 #1 (5′-CAGUUCGGGUGGACUGUCU-3′), SPCS1 #2 (5′-GCAAUA GUUGGAUUUAUCU-3′), SPCS1 #3 (5′-GAUGUUUCAGG-GAAUUAUU-3′), SPCS1 #4 (5′-GUUAUGGCCGGAUUUG-CUU-3′), claudin-1 (5′-CAGUCAAUGCCAGGUACGA-3′), PI4K (5′-GCAAUGUGCUUCGCGAGAA-3′) and scrambled negative control (5′-GCAAGGGAAACCGUGUAAU-3′). Additional control siRNAs for SPCS1 were as follows: C911-#2 (5′-GCAAUAGUaccAUUUAUCU-3′), C911-#3 (5′-GAUGUUU-CuccGAAUUAUU-3′) and C911-#4 (5′-GUUAUGGCgccAUU UGCUU-3′). Bases 9 through 11 of the siRNAs replaced with their complements were shown in lower cases.

Establishment of a stable cell line expressing the shRNA

Huh-7 cells were transfected with pSilencer-SPCS1, and drug-resistant clones were selected by treatment with hygromycin B (Wako, Tokyo, Japan) at a final concentration of 500 μg/ml for 4 weeks.

Virus

HCVtcp and HCVcc derived from JFH-1 having adaptive mutations in E2 (N417S), p7 (N765D), and NS2 (Q1012R) were generated as described previously [33]. The rAT strain of JEV [46] was used to generate virus stock.

Antibodies

Mouse monoclonal antibodies against actin (AC-15) and FLAG (M2) were obtained from Sigma-Aldrich (St. Louis, MO). Mouse

monoclonal antibodies against flavivirus group antigen (D1-4G2) were obtained from Millipore (Billerica, MA). Rabbit polyclonal antibodies against FLAG and V5 were obtained from Sigma-Aldrich. Rabbit polyclonal antibodies against SPCS1, claudin-1, PI4K and myc were obtained from Proteintech (Chicago, IL), Life Technologies (Carlsbad, CA), Cell Signaling (Danvers, MA) and Santa Cruz Biotechnology (Santa Cruz, CA), respectively. An anti-apoE goat polyclonal antibody was obtained from Millipore. Rabbit polyclonal antibodies against NS2 and NS3 were generated with synthetic peptides as antigens. Mouse monoclonal antibodies against HCV Core (2H9) and E2 (8D10-3) and rabbit polyclonal antibodies against NS5A and JEV are described elsewhere [47].

Titration

To determine the titers of HCVcc, Huh7.5.1 cells in 96-well plates were incubated with serially-diluted virus samples and then replaced with media containing 10% FBS and 0.8% carboxymethyl cellulose. Following incubation for 72 h, the monolayers were fixed and immunostained with the anti-NS5A antibody, followed by an Alexa Fluor 488-conjugated anti-rabbit secondary antibody (Invitrogen). Stained foci were counted and used to calculate the titers of focus-forming units (FFU)/ml. For intracellular infectivity of HCVcc, the pellets of infected cells were resuspended in culture medium and were lysed by four freeze-thaw cycles. After centrifugation for 5 min at 4,000 rpm, supernatants were collected and used for virus titration as above. For titration of JEV, Huh7.5.1 cells were incubated with serially-diluted virus samples and then replaced with media containing 10% FBS and 0.8% carboxymethyl cellulose. After a 24 h incubation, the monolayers were fixed and immunostained with a mouse monoclonal anti-flavivirus group antibody (D1-4G2), followed by an Alexa Fluor 488-conjugated anti-mouse secondary antibody (Invitrogen).

Immunoprecipitation

Transfected cells were washed with ice-cold PBS, and suspended in lysis buffer (20 mM Tris-HCl [pH 7.4] containing 135 mM NaCl, 1% TritonX-100, and 10% glycerol) supplemented with 50 mM NaF, 5 mM Na_3VO_4, and complete protease inhibitor cocktail, EDTA free (Roche). Cell lysates were sonicated for 10 min and then incubated for 30 min at 4°C, followed by centrifugation at 14,000× *g* for 10 min. The supernatants were immunoprecipitated with anti-Myc-agarose beads (sc-40, Santa Cruz Biotechnology) or anti-FLAG antibody in the presence of Dynabeads Protein G (Invitrogen). The immunocomplexes were precipitated with the beads by centrifugation at 800× *g* for 30 s, or by applying a magnetic field, and then were washed four times with the lysis buffer. The proteins binding to the beads were boiled with SDS sample buffer and then subjected to SDS–polyacrylamide gel electrophoresis (PAGE).

Immunoblotting

Transfected cells were washed with PBS and lysed with 50 mM Tris-HCl, pH 7.4, 300 mM NaCl, 1% Triton X-100. Lysates were then sonicated for 10 min and added to the same volume of SDS sample buffer. The protein samples were boiled for 10 min, separated by SDS-PAGE, and transferred to polyvinylidene difluoride membranes (Millipore). After blocking, the membranes were probed with the primary antibodies, followed by incubation with peroxidase-conjugated secondary antibody. Antigen-antibody complexes were visualized by an enhanced chemiluminescence detection system (Super Signal West Pico Chemiluminescent Substrate; PIERCE, Rockford, IL) according to the manufacturer's protocol and were detected by an LAS-3000 image analyzer system (Fujifilm, Tokyo, Japan).

Albumin measurement

To determine the human albumin level secreted from cells, culture supernatants were collected and passed through a 0.45-μm pore filter to remove cellular debris. The amounts of human albumin were quantified using a human albumin ELISA kit (Bethyl Laboratories, Montgomery, TX) according to the manufacturer's protocol.

Supporting Information

Figure S1 Effects of SPCS1-siRNAs and the C911 mismatch control siRNAs on the expression of SPCS1 and production of HCV. (A) Huh7.5.1 cells were transfected with either siRNAs targeted for SPCS1 (SPCS1-#2, -#3, and -#4), scrambled control siRNA (Scrambled) or C911 siRNA in which bases 9 through 11 of each SPCS1 siRNA were replaced with their complements (C911-#2, -#3, and -#4) at a final concentration of 15 nM, and were infected with HCVcc at a multiplicity of infection (MOI) of 0.05 at 24 h post-transfection. Expression levels of endogenous SPCS1 and actin in the cells were examined by immunoblotting using anti-SPCS1 and anti-actin antibodies at 3 days post-infection. (B) Infectious titers of HCVcc in the supernatant of the infected cells were determined at 3 days postinfection.
(TIF)

Figure S2 293T cells were transfected with E2 expression plasmid in the presence or absence of SPCS1-myc expression plasmid. The cell lysates of the transfected cells were immunoprecipitated with anti-myc antibody. The resulting precipitates and whole cell lysates used in IP were examined by immunoblotting using anti-E2 or anti-myc antibody. An empty plasmid was used as a negative control.
(TIF)

Figure S3 Interaction of HCV E2 with SPCS1 in mammalian cells. (A) 293T cells were transfected with indicated plasmids. 2 days posttransfection, cells were fixed and permeabilized with Triton X-100, then subjected to in situ PLA (Upper) or immunofluorescence staining (Lower) using anti-FLAG and anti-V5 antibodies. (B) Detection of the SPCS1-E2 interaction in transfected cells using the mKG system. 293T cells were transfected by indicated pair of mKG fusion constructs. Twenty-four hours after transfection, cell were fixed and stained with DAPI, and observed under a confocal microscope.
(TIF)

Acknowledgments

We are grateful to Francis V. Chisari (The Scripps Research Institute) for providing Huh7.5.1 cells, and Drs. C.K. Lim and T. Takasaki (National Institute of Infectious Diseases) for providing rabbit polyclonal anti-JEV antibodies. We thank M. Sasaki and T. Date for their technical assistance, and T. Mizoguchi for secretarial work. We also thank H. Hasegawa, T. Kato, T. Masaki, N. Watanabe, and A. Murayama for their helpful discussions.

Author Contributions

Conceived and designed the experiments: RS TS. Performed the experiments: RS MM. Analyzed the data: RS KW HA TS. Contributed reagents/materials/analysis tools: YM TW. Wrote the paper: RS TS.

References

1. Hoofnagle JH (2002) Course and outcome of hepatitis C. Hepatology 36: S21–29.
2. Suzuki T, Aizaki H, Murakami K, Shoji I, Wakita T (2007) Molecular biology of hepatitis C virus. J Gastroenterol 42: 411–423.
3. Appel N, Zayas M, Miller S, Krijnse-Locker J, Schaller T, et al. (2008) Essential role of domain III of nonstructural protein 5A for hepatitis C virus infectious particle assembly. PLoS Pathog 4: e1000035.
4. Dentzer TG, Lorenz IC, Evans MJ, Rice CM (2009) Determinants of the hepatitis C virus nonstructural protein 2 protease domain required for production of infectious virus. J Virol 83: 12702–12713.
5. Jirasko V, Montserret R, Appel N, Janvier A, Eustachi L, et al. (2008) Structural and functional characterization of nonstructural protein 2 for its role in hepatitis C virus assembly. J Biol Chem 283: 28546–28562.
6. Jones CT, Murray CL, Eastman DK, Tassello J, Rice CM (2007) Hepatitis C virus p7 and NS2 proteins are essential for production of infectious virus. J Virol 81: 8374–8383.
7. Ma Y, Yates J, Liang Y, Lemon SM, Yi M (2008) NS3 helicase domains involved in infectious intracellular hepatitis C virus particle assembly. J Virol 82: 7624–7639.
8. Masaki T, Suzuki R, Murakami K, Aizaki H, Ishii K, et al. (2008) Interaction of hepatitis C virus nonstructural protein 5A with core protein is critical for the production of infectious virus particles. J Virol 82: 7964–7976.
9. Tellinghuisen TL, Foss KL, Treadaway J (2008) Regulation of hepatitis C virion production via phosphorylation of the NS5A protein. PLoS Pathog 4: e1000032.
10. Phan T, Beran RK, Peters C, Lorenz IC, Lindenbach BD (2009) Hepatitis C virus NS2 protein contributes to virus particle assembly via opposing epistatic interactions with the E1–E2 glycoprotein and NS3-NS4A enzyme complexes. J Virol 83: 8379–8395.
11. Lorenz IC, Marcotrigiano J, Dentzer TG, Rice CM (2006) Structure of the catalytic domain of the hepatitis C virus NS2-3 protease. Nature 442: 831–835.
12. Lohmann V, Korner F, Koch J, Herian U, Theilmann L, et al. (1999) Replication of subgenomic hepatitis C virus RNAs in a hepatoma cell line. Science 285: 110–113.
13. Kato T, Choi Y, Elmowalid G, Sapp RK, Barth H, et al. (2008) Hepatitis C virus JFH-1 strain infection in chimpanzees is associated with low pathogenicity and emergence of an adaptive mutation. Hepatology 48: 732–740.
14. Scheel TK, Gottwein JM, Jensen TB, Prentoe JC, Hoegh AM, et al. (2008) Development of JFH1-based cell culture systems for hepatitis C virus genotype 4a and evidence for cross-genotype neutralization. Proc Natl Acad Sci U S A 105: 997–1002.
15. Jensen TB, Gottwein JM, Scheel TK, Hoegh AM, Eugen-Olsen J, et al. (2008) Highly efficient JFH1-based cell-culture system for hepatitis C virus genotype 5a: failure of homologous neutralizing-antibody treatment to control infection. J Infect Dis 198: 1756–1765.
16. Yi M, Ma Y, Yates J, Lemon SM (2007) Compensatory mutations in E1, p7, NS2, and NS3 enhance yields of cell culture-infectious intergenotypic chimeric hepatitis C virus. J Virol 81: 629–638.
17. Russell RS, Meunier JC, Takikawa S, Faulk K, Engle RE, et al. (2008) Advantages of a single-cycle production assay to study cell culture-adaptive mutations of hepatitis C virus. Proc Natl Acad Sci U S A 105: 4370–4375.
18. Popescu CI, Callens N, Trinel D, Roingeard P, Moradpour D, et al. (2011) NS2 protein of hepatitis C virus interacts with structural and non-structural proteins towards virus assembly. PLoS Pathog 7: e1001278.
19. Ma Y, Anantpadma M, Timpe JM, Shanmugam S, Singh SM, et al. (2011) Hepatitis C virus NS2 protein serves as a scaffold for virus assembly by interacting with both structural and nonstructural proteins. J Virol 85: 86–97.
20. Stapleford KA, Lindenbach BD (2011) Hepatitis C virus NS2 coordinates virus particle assembly through physical interactions with the E1–E2 glycoprotein and NS3-NS4A enzyme complexes. J Virol 85: 1706–1717.
21. Jirasko V, Montserret R, Lee JY, Gouttenoire J, Moradpour D, et al. (2010) Structural and functional studies of nonstructural protein 2 of the hepatitis C virus reveal its key role as organizer of virion assembly. PLoS Pathog 6: e1001233.
22. Yi M, Ma Y, Yates J, Lemon SM (2009) Trans-complementation of an NS2 defect in a late step in hepatitis C virus (HCV) particle assembly and maturation. PLoS Pathog 5: e1000403.
23. Counihan NA, Rawlinson SM, Lindenbach BD (2011) Trafficking of hepatitis C virus core protein during virus particle assembly. PLoS Pathog 7: e1002302.
24. Kiiver K, Merits A, Ustav M, Zusinaite E (2006) Complex formation between hepatitis C virus NS2 and NS3 proteins. Virus Res 117: 264–272.
25. Selby MJ, Glazer E, Masiarz F, Houghton M (1994) Complex processing and protein:protein interactions in the E2:NS2 region of HCV. Virology 204: 114–122.
26. Johnsson N, Varshavsky A (1994) Split ubiquitin as a sensor of protein interactions in vivo. Proc Natl Acad Sci U S A 91: 10340–10344.
27. Evans E, A., Gilmore R, Blobel G (1986) Purification of microsomal signal peptidase as a complex. Proc Natl Acad Sci U S A 83: 581–585.
28. Fang H, Panzner S, Mullins C, Hartmann E, Green N (1996) The homologue of mammalian SPC12 is important for efficient signal peptidase activity in Saccharomyces cerevisiae. J Biol Chem 271: 16460–16465.
29. Wakita T, Pietschmann T, Kato T, Date T, Miyamoto M, et al. (2005) Production of infectious hepatitis C virus in tissue culture from a cloned viral genome. Nat Med 11: 791–796.
30. Söderberg O, Gullberg M, Jarvius M, Ridderstrale K, Leuchowius KJ, et al. (2006) Direct observation of individual endogenous protein complexes in situ by proximity ligation. Nat Methods 3: 995–1000.
31. Kerppola TK (2006) Complementary methods for studies of protein interactions in living cells. Nat Methods 3: 969–971.
32. Buehler E, Chen YC, Martin S (2012) C911: A bench-level control for sequence specific siRNA off-target effects. PLoS One 7: e51942.
33. Suzuki R, Saito K, Kato T, Shirakura M, Akazawa D, et al. (2012) Trans-complemented hepatitis C virus particles as a versatile tool for study of virus assembly and infection. Virology 432: 29–38.
34. Chang KS, Jiang J, Cai Z, Luo G (2007) Human apolipoprotein E is required for infectivity and production of hepatitis C virus in cell culture. J Virol 81: 13783–13793.
35. Owen DM, Huang H, Ye J, Gale M, Jr. (2009) Apolipoprotein E on hepatitis C virion facilitates infection through interaction with low-density lipoprotein receptor. Virology 394: 99–108.
36. Akazawa D, Date T, Morikawa K, Murayama A, Miyamoto M, et al. (2007) CD81 expression is important for the permissiveness of Huh7 cell clones for heterogeneous hepatitis C virus infection. J Virol 81: 5036–5045.
37. Erdtmann L, Franck N, Lerat H, Le Seyec J, Gilot D, et al. (2003) The hepatitis C virus NS2 protein is an inhibitor of CIDE-B-induced apoptosis. J Biol Chem 278: 18256–18264.
38. de Chassey B, Navratil V, Tafforeau L, Hiet MS, Aublin-Gex A, et al. (2008) Hepatitis C virus infection protein network. Mol Syst Biol 4: 230.
39. Stagljar I, Korostensky C, Johnsson N, te Heesen S (1998) A genetic system based on split-ubiquitin for the analysis of interactions between membrane proteins in vivo. Proc Natl Acad Sci U S A 95: 5187–5192.
40. Kalies KU, Hartmann E (1996) Membrane topology of the 12- and the 25-kDa subunits of the mammalian signal peptidase complex. J Biol Chem 271: 3925–3929.
41. Mullins C, Meyer HA, Hartmann E, Green N, Fang H (1996) Structurally related Spc1p and Spc2p of yeast signal peptidase complex are functionally distinct. J Biol Chem 271: 29094–29099.
42. Li Q, Brass AL, Ng A, Hu Z, Xavier RJ, et al. (2009) A genome-wide genetic screen for host factors required for hepatitis C virus propagation. Proc Natl Acad Sci U S A 106: 16410–16415.
43. Zhong J, Gastaminza P, Cheng G, Kapadia S, Kato T, et al. (2005) Robust hepatitis C virus infection in vitro. Proc Natl Acad Sci U S A 102: 9294–9299.
44. Masaki T, Suzuki R, Saeed M, Mori K, Matsuda M, et al. (2010) Production of infectious hepatitis C virus by using RNA polymerase I-mediated transcription. J Virol 84: 5824–5835.
45. Suzuki R, Sakamoto S, Tsutsumi T, Rikimaru A, Tanaka K, et al. (2005) Molecular determinants for subcellular localization of hepatitis C virus core protein. J Virol 79: 1271–1281.
46. Zhao Z, Date T, Li Y, Kato T, Miyamoto M, et al. (2005) Characterization of the E-138 (Glu/Lys) mutation in Japanese encephalitis virus by using a stable, full-length, infectious cDNA clone. J Gen Virol 86: 2209–2220.
47. Saeed M, Suzuki R, Watanabe N, Masaki T, Tomonaga M, et al. (2011) Role of the endoplasmic reticulum-associated degradation (ERAD) pathway in degradation of hepatitis C virus envelope proteins and production of virus particles. J Biol Chem 286: 37264–37273.

Zinc-finger antiviral protein mediates retinoic acid inducible gene I–like receptor-independent antiviral response to murine leukemia virus

Hanna Lee[a,b], Jun Komano[c], Yasunori Saitoh[d], Shoji Yamaoka[d], Tatsuya Kozaki[a,b], Takuma Misawa[a,b], Michihiro Takahama[a,b], Takashi Satoh[a,b], Osamu Takeuchi[e], Naoki Yamamoto[f], Yoshiharu Matsuura[g], Tatsuya Saitoh[a,b,1], and Shizuo Akira[a,b,1]

[a]Laboratory of Host Defense, World Premier International Immunology Frontier Research Center, Osaka University, Osaka 565-0871, Japan; Departments of [b]Host Defense and [g]Molecular Virology, Research Institute for Microbial Diseases, Osaka University, Osaka 565-0871, Japan; [c]Department of Infectious Diseases, Osaka Prefectural Institute of Public Health, Osaka 537-0025, Japan; [d]Department of Molecular Virology, Graduate School of Medical and Dental Sciences, Tokyo Medical and Dental University, Tokyo 113-8519, Japan; [e]Laboratory of Infection and Prevention, Institute for Virus Research, Kyoto University, Kyoto 606-8507, Japan; and [f]Department of Microbiology, Yong Loo Lin School of Medicine, National University of Singapore, Singapore 117599

Contributed by Shizuo Akira, June 5, 2013 (sent for review May 14, 2013)

When host cells are infected by an RNA virus, pattern-recognition receptors (PRRs) recognize the viral RNA and induce the antiviral innate immunity. Toll-like receptor 7 (TLR7) detects the genomic RNA of incoming murine leukemia virus (MLV) in endosomes and mediates the antiviral response. However, the RNA-sensing PRR that recognizes the MLV in the cytosol is not fully understood. Here, we definitively demonstrate that zinc-finger antiviral protein (ZAP) acts as a cytosolic RNA sensor, inducing the degradation of the MLV transcripts by the exosome, an RNA degradation system, on RNA granules. Although the retinoic acid inducible gene I (RIG-I)–like receptors (RLRs) RIG-I and melanoma differentiation-associated protein 5 detect various RNA viruses in the cytosol and induce the type I IFN-dependent antiviral response, RLR loss does not alter the replication efficiency of MLV. In sharp contrast, the loss of ZAP greatly enhances the replication efficiency of MLV. ZAP localizes to RNA granules, where the processing-body and stress-granule proteins assemble. ZAP induces the recruitment of the MLV transcripts and exosome components to the RNA granules. The CCCH-type zinc-finger domains of ZAP, which are RNA-binding motifs, mediate its localization to RNA granules and MLV transcripts degradation by the exosome. Although ZAP was known as a regulator of RIG-I signaling in a human cell line, ZAP deficiency does not affect the RIG-I–dependent production of type I IFN in mouse cells. Thus, ZAP is a unique member of the cytosolic RNA-sensing PRR family that targets and eliminates intracellular RNA viruses independently of TLR and RLR family members.

host defense | retrovirus | ZC3HAV1

Innate immunity is induced after the recognition of viral RNAs by pattern-recognition receptors (PRRs) and is the first line of the host defenses against a variety of RNA viruses (1, 2). Among the PRRs, the Toll-like receptor (TLR) and retinoic acid-inducible gene I (RIG-I)-like receptor (RLR) families play major roles in the recognition of viral RNAs. The RLR's RIG-I [also called DEAD (Asp-Glu-Ala-Asp) box polypeptide 58 (DDX58)] and melanoma differentiation-associated protein 5 [MDA5, also called interferon induced with helicase C domain 1 (IFIH1)] are RNA helicases that sense the ds form of viral RNAs in the cytosol (3, 4). After sensing dsRNA, the RLRs trigger a signaling pathway that activates interferon (IFN) regulatory factor 3 (IRF3) and IRF7, transcription factors that induce IFN stimulation-responsive, element-dependent transcription (5, 6). This results in the production of type I IFN and the expression of IFN-inducible antiviral proteins. The sensing of viral RNAs by TLR family members also induces the IRF3- and IRF7-dependent type I IFN response (1, 2). In epithelial cells, TLR3, a sensor of dsRNA, detects the incoming RNA virus genomes in endosomes and induces the activation of IRF3, leading to the production of type I IFN (7, 8). In plasmacytoid dendritic cells, TLR7, a sensor of single-stranded (ss) RNA, detects incoming RNA virus genomes in endo-lysosomes and triggers the activation of IRF7, leading to the robust production of type I IFN (9–13). Thus, TLRs and RLRs play major roles in the establishment of an antiviral state by mediating the production of type I IFN.

Murine leukemia virus (MLV), a retrovirus belonging to the gammaretroviral genus of the family *Retroviridae*, is a causative agent of cancer in murine hosts (14, 15). Although type I IFN is essential for the protection of hosts from lethal infection with a variety of RNA viruses, such as influenza A virus (IAV) and vesicular stomatitis virus (VSV), type I IFN is not essential for induction of the antiviral state against MLV (16–18). Therefore, a different type of innate immune system has been proposed to protect hosts from MLV infection. Although TLR7 has been shown to induce virus-neutralizing immunity after MLV genomic RNA is detected in endosomes (16), the RNA sensor responsible for the elimination of MLV in the cytosol has not been fully understood. RLRs are candidate RNA sensors of intracellular MLV. RLRs might mediate the antiviral response to MLV after the viral RNA is detected, independently of type I IFN because RLRs stimulate not only IRF3/IRF7, but also other transcription factors, such as NF-κB and activator protein 1, which are responsible for the production of inflammatory cytokines and chemokines (19). Another candidate sensor is zinc-finger antiviral protein [ZAP, also called zinc finger CCCH-type, antiviral 1 (ZC3HAV1)]. ZAP was originally identified with an expression cloning method as one of the antiviral proteins directed against MLV (20). ZAP reduces the level of MLV transcripts in the cytosol to suppress MLV infection at the posttranscriptional stage, whereas ZAP does not inhibit the early stage of the MLV infection. ZAP recognizes the MLV transcripts via its CCCH-type zinc-finger domains and binds with RNA helicases and the components of the exosome (an RNA degradation system) to induce the degradation of the MLV transcripts (21–25). However, it is unclear whether endogenous ZAP is involved in the antiviral response to replication-competent MLV in primary cells. In the present study, we examined the roles of these two types of cytosolic RNA sensors and demonstrated the spatial regulation of the innate immune response directed against intracellular MLV.

Author contributions: T. Saitoh and S.A. designed research; H.L., J.K., Y.S., S.Y., T.K., T.M., M.T., T. Satoh, O.T., N.Y., and Y.M. performed research; and T. Saitoh wrote the paper.

The authors declare no conflict of interest.

[1]To whom correspondence may be addressed. E-mail: sakira@biken.osaka-u.ac.jp or tatsuya@biken.osaka-u.ac.jp.

This article contains supporting information online at www.pnas.org/lookup/suppl/doi:10.1073/pnas.1310604110/-/DCSupplemental.

Results

RLRs Do Not Regulate the Antiviral Response to MLV in Primary Mouse Embryonic Fibroblasts. We first examined the involvement of RLRs in the antiviral response to MLV in mouse embryonic fibroblasts (MEFs). The replication efficiency of MLV in *Ddx58*$^{-/-}$/*Ifih1*$^{-/-}$ MEFs was similar to that in *Ddx58*$^{+/+}$/*Ifih1*$^{+/+}$ MEFs (Fig. 1*A*). Furthermore, the replication efficiency of MLV in *Irf3*$^{-/-}$/*Irf7*$^{-/-}$ MEFs was similar to that in *Irf3*$^{+/-}$/*Irf7*$^{+/-}$ MEFs (Fig. 1*B*). Consistent with this, the levels of *Ifnb1* and *chemokine (C-X-C motif) ligand 10* (*Cxcl10*) mRNAs did not change during MLV infection (Fig. 1 *C–F*). The RLR–IRF3/7 signaling axis is essential for the up-regulation of *Ifnb1* and *Cxcl10* mRNAs during VSV infection. R848, a ligand of TLR7, failed to stimulate MEFs isolated from C57BL/6 mice (Fig. S1), indicating that no RNA-sensing TLR family member recognizes MLV in the extracellular space of MEFs. Therefore, MLV evades the RLR and TLR systems and does not induce the type I IFN response in MEFs.

Endogenous ZAP Limits the Replication of MLV in Primary MEFs. We next investigated the role of ZAP, another cytosolic sensor of viral RNA, in the antiviral response to MLV. Previous studies have demonstrated that the ectopic expression of ZAP potently inhibits replication-incompetent MLV in the cytoplasm of various types of cell lines (20). Therefore, we generated *Zc3hav1*$^{-/-}$ mice to examine whether endogenous ZAP controls the replication of MLV in primary cells (Fig. S2). Detectable levels of ZAP protein were expressed in *Zc3hav1*$^{+/+}$ MEFs before and after MLV infection (Fig. S2*D*). Whereas ZAP deficiency did not alter the replication efficiency of VSV in MEFs (Fig. S3), ZAP deficiency greatly enhanced the replication efficiency of MLV (Fig. 2 *A* and *B*). These findings indicate that endogenous ZAP is responsible for the antiviral response to replication-competent MLV in primary mouse cells.

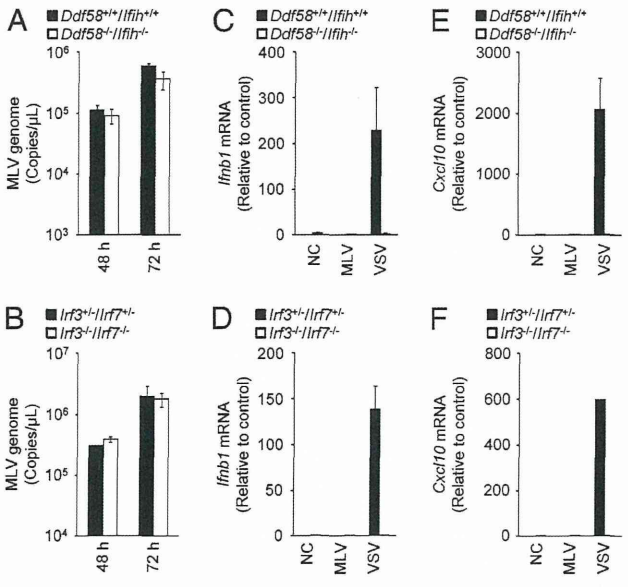

Fig. 1. RIG-I–like receptors are not essential for the antiviral response to MLV in primary MEFs. (*A* and *B*) *Ddx58*$^{+/+}$/*Ifih1*$^{+/+}$ and *Ddx5*$^{-/-}$/*Ifih1*$^{-/-}$ MEFs (*A*) or *Irf3*$^{+/-}$/*Irf7*$^{+/-}$ and *Irf*$^{-/-}$/*Irf7*$^{-/-}$ MEFs (*B*) were infected with MLV (2×10^{10} copies per μL) for 48 or 72 h. The copy numbers of the MLV genome in the culture supernatants were measured by quantitative RT-PCR. (*C–F*) *Ddx58*$^{+/+}$/*Ifih1*$^{+/+}$ and *Ddx58*$^{-/-}$/*Ifih1*$^{-/-}$ MEFs (*C* and *E*) or *Irf3*$^{+/-}$/*Irf7*$^{+/-}$ and *Irf3*$^{-/-}$/*Irf7*$^{-/-}$ MEFs (*D* and *F*) were infected with MLV (2×10^{10} copies per μL) or VSV [multiplicity of infection (MOI) = 1] for 12 h. The levels of *Ifnb1* (*C* and *D*) and *Cxcl10* (*E* and *F*) mRNAs were measured by quantitative RT-PCR. The results shown are means ± SD ($n = 3$).

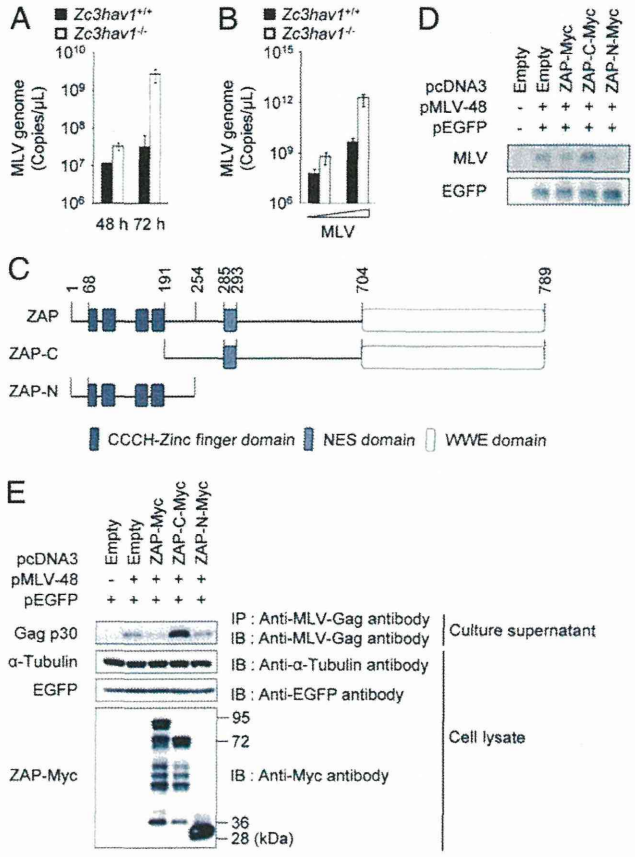

Fig. 2. ZAP inhibits MLV replication in primary MEFs. (*A*) *Zc3hav1*$^{+/+}$ and *Zc3hav1*$^{-/-}$ MEFs were infected with MLV (2×10^{10} copies per μL). Viral RNA was isolated at the indicated time points. The copy numbers of the MLV genome in the culture supernatants were measured by quantitative RT-PCR. (*B*) *Zc3hav1*$^{+/+}$ and *Zc3hav1*$^{-/-}$ MEFs were infected with increasing doses of MLV (2×10^{8} and 2×10^{9} copies per μL) for 96 h. The copy numbers of the MLV genome in the culture supernatants were measured by quantitative RT-PCR. (*C*) Domain architecture of ZAP. (*D* and *E*) 293T cells were transfected with pMLV-48 and pEGFP-N1 together with the indicated ZAP expression plasmids for 48 h. Cytoplasmic RNA was subjected to Northern blotting analysis of the indicated RNAs (*D*). The culture supernatants were subjected to immunoprecipitation coupled to immunoblotting to detect the indicated proteins (*E*). The results shown are means ± SD ($n = 3$). NES, nuclear export signal.

The CCCH-type zinc-finger domains of ZAP are known to recognize the MLV transcripts and to induce its degradation (21, 25). Consistent with this, the ectopic expression of the N-terminal portion of ZAP, which contains the CCCH-type zinc-finger domains, but not the ectopic expression of the C-terminal portion of ZAP, which lacks CCCH-type zinc-finger domains, reduced the level of MLV transcripts in the cytosol (Fig. 2 *C* and *D*). The ectopic expression of the CCCH-type zinc-finger domains of ZAP also suppressed the expression of the Gag protein of MLV (Fig. 2*E*). Therefore, the CCCH-type zinc-finger domains of ZAP are essential for its antiviral action against MLV.

CCCH-Type Zinc-Finger Domains of ZAP Mediate Its Localization to the RNA Granules. The involvement of ZAP in the antiviral response to MLV prompted us to determine the mechanism underlying the ZAP-dependent degradation of the MLV transcripts. Although a previous study showed that ZAP acts in the cytosol (20), it was still unclear where in the cytosol ZAP eliminates the MLV transcripts. Therefore, we examined whether ZAP localizes to a cytosolic compartment, such as in the processing bodies

(P-bodies) (26). When it was ectopically expressed, ZAP localized to cytoplasmic dot-like structures in a manner that was dependent on its CCCH-type zinc-finger domains (Fig. 3*A*). The ZAP-positive dot-like structures colocalized with marker proteins for P-bodies, such as DCP1 decapping enzyme homolog A (*Saccharomyces cerevisiae*; DCP1A) and DDX6 (Fig. 3*B*). ZAP induced the enlargement of the DCP1A- and DDX6-positive dot-like structures, suggesting that the ZAP-positive dot-like structures are not conventional P-bodies. ZAP also colocalized with marker proteins for stress granules, such as GTPase-activating protein (SH3 domain) binding protein 1 (G3BP1) and cytotoxic granule-associated RNA binding protein (TIA-1) (Fig. S4). Furthermore, the RNA helicase DEAH (Asp-Glu-Ala-His) box polypeptide 30 (DHX30), which binds to ZAP to facilitate its antiviral action against MLV (24), colocalized with ZAP to the DCP1A-positive dot-like structures (Fig. S5). By contrast, ZAP did not colocalize with mitochondrial preprotein translocases of the outer membrane 20 (TOM20), 70-kDa peroxisomal membrane protein (PMP70), early endosome antigen 1 (EEA1), or lysosomal-associated membrane protein 1 (LAMP1), marker proteins for the mitochondria, peroxisomes, endosomes, and lysosomes, respectively (Fig. 3*C*). These findings indicate that ZAP localizes to the RNA granules, where the marker proteins for P-bodies and stress granules assemble.

ZAP Recruits the MLV Transcripts and Exosome Components to RNA Granules. The localization of the MLV transcripts has been poorly understood. We used an improved RNA FISH method to visualize the subcellular localization of viral RNA and identified the cytosolic compartments in which ZAP acts on the MLV transcripts. The MLV transcripts mainly localize in the cytosol and colocalize with DCP1A-positive RNA granules at low frequency (Fig. 4). However, the ectopic expression of ZAP reduced the level of MLV transcripts in the cytosol and dramatically altered its localization from the cytosol to ZAP- and DCP1A-positive RNA granules (Fig. 4 and Fig. S6). Therefore, ZAP tethers the MLV transcripts and transfers it to the RNA granules.

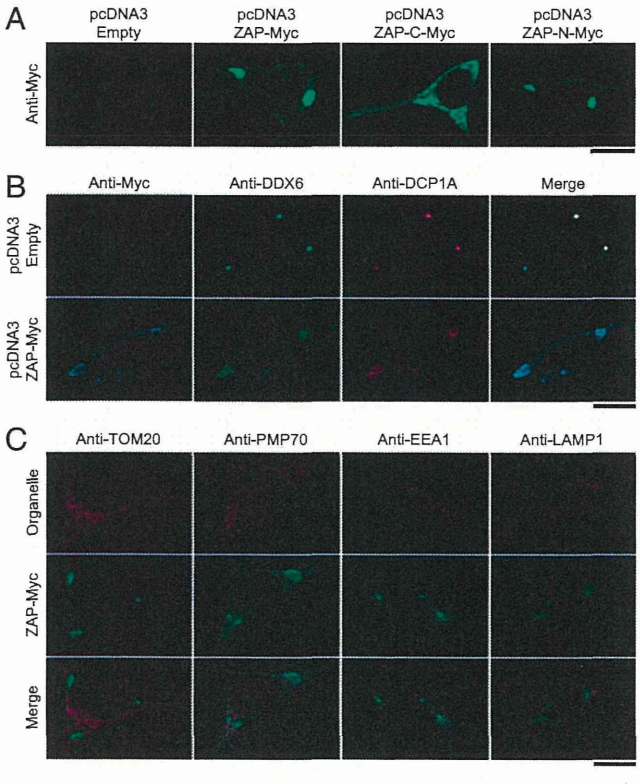

Fig. 3. ZAP localizes to DCP1A- and DDX6-positive RNA granules. (*A–C*) 293T cells were transfected with the indicated vectors for 48 h and then fixed. The samples were immunostained with the indicated antibodies and then observed by confocal laser scanning microscopy. The data are representative of three independent experiments. (Scale bars, 10 μm.)

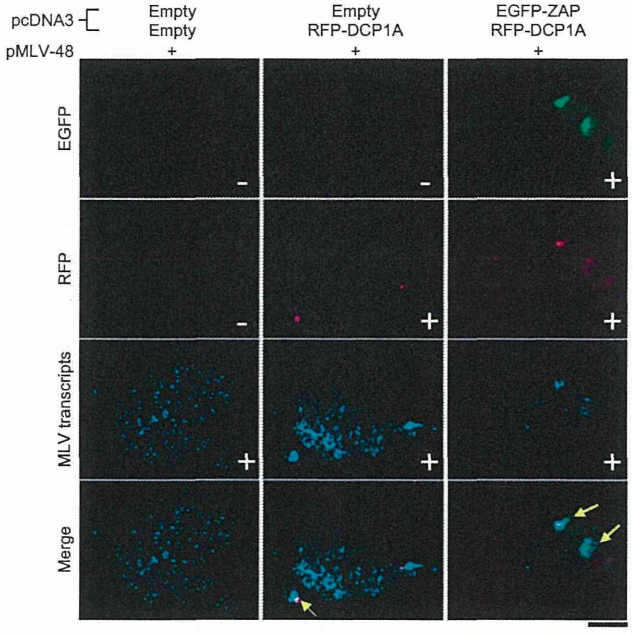

Fig. 4. ZAP recruits the MLV transcripts to RNA granules. 293T cells were transfected with the indicated plasmids for 48 h and then fixed. The samples were subjected to in situ hybridization analysis with a fluorescent probe for MLV transcripts and then observed by confocal laser scanning microscopy. (Scale bar, 10 μm.)

Because ZAP is not a ribonuclease, it requires the support of an RNA degradation system to destabilize the MLV transcripts. Consistent with this, previous studies have shown that exosome components and RNA helicases interact with ZAP to mediate the antiviral response to MLV (22–24). Therefore, we focused on the localization of exosome component 5 (EXOSC5, also known as RRP46) (27). The ectopic expression of EXOSC5 reduced the level of MLV transcripts in the cytosol (Fig. 5*A*). Under normal conditions, EXOSC5 localized in the cytosol and nuclei, and colocalized with the DCP1A-positive RNA granules at low frequency (Fig. 5*B*). However, when ZAP was ectopically expressed, EXOSC5 moved from the cytosol to the ZAP- and DCP1A-positive RNA granules (Fig. 5*B*). These findings indicate that ZAP recruits the exosome component to the RNA granules to induce the degradation of MLV transcripts.

ZAP Does Not Regulate the RIG-I–Dependent Type I IFN Response in Primary Mouse Cells. A recent study showed that ZAP positively regulated RIG-I signaling during RNA virus infection in a human cell line (28). Therefore, we examined the involvement of ZAP in the RIG-I–dependent type I IFN response in primary mouse cells. In *Zc3hav1*$^{-/-}$ primary MEFs, the IFN-β and Cxcl10 proteins were produced normally in response to VSV, an RNA virus recognized by RIG-I (Fig. 6 *A* and *B*). Although ZAP deficiency greatly enhanced the replication of MLV (Fig. 2 *A* and *B*), no IFN-β or Cxcl10 protein was produced in *Zc3hav1*$^{-/-}$ MEFs infected with MLV. In *Zc3hav1*$^{-/-}$ mouse primary dendritic cells, IFN-β and Cxcl10 were also normally produced in response to

IMMUNOLOGY

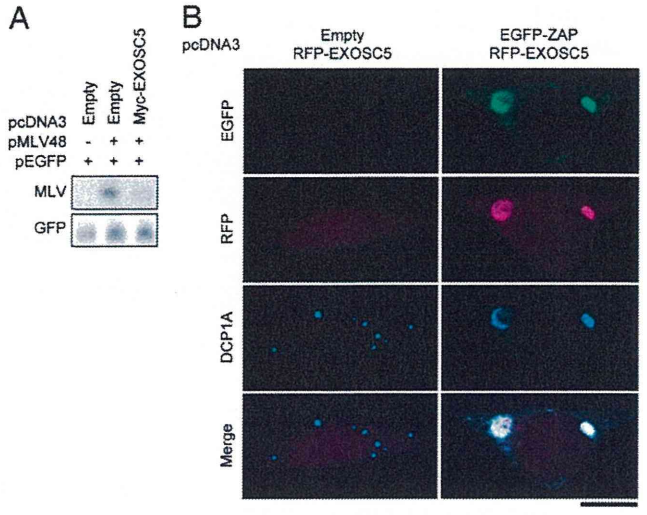

Fig. 5. EXOSC5 colocalizes with ZAP on RNA granules. (*A*) 293T cells were transfected with pMLV-48 and pEGFP-N1 together with the indicated ZAP expression plasmids for 48 h. Cytoplasmic RNA was subjected to Northern blotting analysis to detect the indicated RNAs. (*B*) 293T cells were transfected with the indicated plasmids and then fixed. The samples were immunostained with anti-DCP1A antibody and then observed by confocal laser scanning microscopy. The data are representative of three independent experiments. (Scale bar, 10 μm.)

Newcastle disease virus (NDV) and IAV, RNA viruses recognized by RIG-I (Fig. 6 *C* and *D*). Furthermore, ZAP deficiency did not affect the production of IFN-β in MEFs stimulated with the RIG-I ligand, 5′ triphosphate dsRNA (3pRNA) (Fig. S7 *A* and *B*), the MDA5 ligand poly(rI–rC), and a synthetic dsDNA poly(dA–dT) (Fig. S7*C*). These findings indicate that ZAP is not a regulator of the RIG-I–dependent type I IFN response in primary mouse cells and strengthen our conclusion that ZAP eliminates MLV independently of the RLR–IRF3/7 signaling axis.

Discussion

In this study, we showed that endogenous ZAP suppresses the replication of MLV in MEFs. This raises the issue of whether endogenous ZAP suppresses the replication of other types of RNA viruses, including human retroviruses. The RNAi-mediated knockdown of *ZC3HAV1* mRNA enhanced the replication of xenotropic MLV-related virus, an artificial retrovirus belonging to the gammaretroviral genus of the family *Retroviridae* (29), in 293T cells (Fig. S8 *A* and *B*), whereas the knockdown of *ZC3HAV1* mRNA did not enhance the replication of human T-cell leukemia virus type I, a retrovirus belonging to the deltaretroviral genus of the family *Retroviridae* (30), in MT-2 cells (Fig. S8 *C* and *D*). In a previous study, the knockdown of *ZC3HAV1* mRNA enhanced the replication of HIV-1, a retrovirus belonging to the lentiviral genus of the family *Retroviridae* (31), in HOS-CD4 cells expressing chemokine (C-C motif) receptor 5 (32). Therefore, ZAP functions in human cells to target not all but certain types of retroviruses. ZAP is also known to suppress the replication of RNA viruses belonging to the families *Filoviridae* and *Togaviridae* (33, 34). Although ZAP has been shown to recognize the viral RNA of RNA viruses belonging to the families *Filoviridae*, *Togaviridae*, and *Retroviridae via*, its CCCH-type zinc-finger domains, the common features that are recognized by these domains, such as specific sequences or structural characteristics, have not been determined. Further studies are required to identify the RNA ligand of ZAP that induces the destabilization of the viral RNA by the RNA degradation machinery.

Although accumulating evidence indicates that ZAP counters a variety of RNA viruses under in vitro experimental conditions (20, 33, 34), it is still unclear whether ZAP protects hosts from RNA viral infections in vivo. RNA-sensing TLRs and the ssDNA cytosine deaminase apolipoprotein B mRNA-editing, enzyme-catalytic, polypeptide-like 3 are other antiviral systems that affect mouse retroviruses, and also control the replication of endogenous retroviruses (ERVs) (16, 35–37). Therefore, ZAP might also contribute to the antiviral response to ERVs and prevent the ERV-induced generation of tumors in vivo. To assess this, we are now establishing a colony of *Zc3hav1*$^{-/-}$ mice in the C57BL/6 genetic background. In a future study, we will attempt to determine the in vivo role of ZAP in the host defense responses to endogenous and exogenous microbes.

The CCCH-type zinc-finger–domain-containing protein family regulates RNA synthesis, splicing, and degradation, and is involved in a variety of cellular events, including cell growth, cell death, the inflammatory response, and the antimicrobial response (38, 39). To date, more than 50 CCCH-type zinc-finger-domain–containing proteins have been identified (40). Although various CCCH-type zinc-finger-domain-containing proteins, including tristetraprolin, roquin, and regnase-1, have been shown to be regulators of cytokine mRNA stability, ZAP is the only CCCH-type zinc-finger–domain-containing protein known to promote the destabilization of viral RNA (20, 41–43). Therefore, it will be interesting to identify a CCCH-type zinc-finger–domain-containing protein capable of mediating an antiviral response to RNA viruses that have evaded ZAP and the other RNA-sensing PRRs.

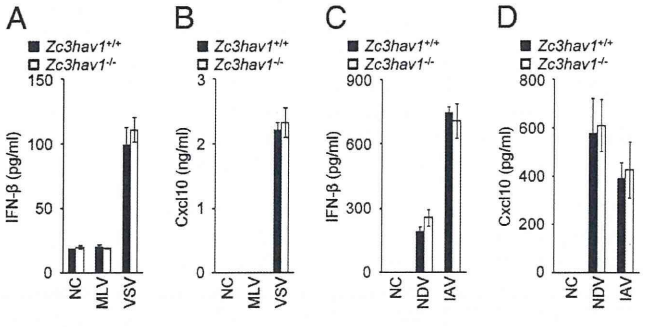

Fig. 6. ZAP is not essential for the RIG-I–mediated type I IFN response. (*A* and *B*) *Zc3hav1*$^{+/+}$ and *Zc3hav1*$^{-/-}$ MEFs were infected with MLV (2×10^{10} copies per μL) or VSV (MOI = 1) for 12 h. The levels of IFN-β (*A*) and Cxcl10 (*B*) proteins in the culture supernatants were measured with ELISAs. (*C* and *D*) *Zc3hav1*$^{+/+}$ and *Zc3hav1*$^{-/-}$ bone marrow-derived dendritic cells were infected with NDV (2.5×10^5 pfu/mL) or IAV (PR8, 100 Hematoglutinin) for 24 h. The levels of IFN-β (*C*) and Cxcl10 (*D*) proteins in the culture supernatants were measured with ELISAs. The results shown are means ± SD ($n = 3$).

Materials and Methods

Reagents. Anti-MLV-Gag antibody (ABIN457547) was purchased from Antibodies-online. Anti–α-tubulin antibody (T6199) was purchased from Sigma. Anti-GFP antibody (598) was purchased from MBL. Chicken anti–avian myelocytomatosis viral oncogene homolog (Myc) antibody (A190-103A) for the immunostaining assay was purchased from Bethyl Laboratories. Mouse anti–Myc-tag antibody (2276S) for immunoblotting was purchased from Cell Signaling. Anti-DDX6 (ab40684), anti-PMP70 (ab3421), and anti-LAMP1 (ab24170) antibodies were purchased from Abcam. Anti-DCP1A antibody (H00055802-M06) was purchased from Abnova. Anti-TOM20 antibody (SC-11415) was purchased from Santa Cruz Biotechnology. Anti-EEA1 antibody (610456) was purchased from BD Biosciences. The ELISA kit for mouse IFN-β was purchased from Pestka Biomedical Laboratories Interferon Source. The ELISA kit for mouse Cxcl10 was purchased from R&D Systems.

Plasmids. pMLV-48 (GenBank accession no. J02255.1) was previously described (44) and kindly donated by H. Fan (University of California, Irvine, CA). pcDNA3.1(+) was purchased from Invitrogen. To generate the ZAP

expression constructs, NheI/NotI cDNA fragments encoding full-length mouse ZAP (GenBank accession no. NM_028864.2) and the C-terminal portion of ZAP and a BamHI/NotI cDNA fragment encoding the N-terminal portion of ZAP were amplified from pCMV–SPORT6–Zc3hav1 (MMM1013-7511214, Open Biosystems) by PCR and cloned into the corresponding restriction sites of pcDNA3 to produce pcDNA3–ZAP, pcDNA3–ZAP–C, and pcDNA3–ZAP–N, respectively. To generate the expression construct for the EGFP–ZAP fusion protein, an NheI/SpeI cDNA fragment encoding EGFP was amplified from pEGFP-N1 (Clontech) by PCR and cloned into the NheI site of pcDNA3–ZAP to produce pcDNA3–EGFP–ZAP. To generate the red fluorescent protein (RFP) expression construct, a BamHI/EcoRI cDNA fragment of RFP was amplified from pTagRFP-N1 (Evrogen) by PCR and cloned into the BamHI/EcoRI sites of pcDNA3 to produce pcDNA3–RFP. To generate the expression constructs for the RFP–DCP1A and RFP–EXOSC5 fusion proteins, EcoRI/NotI cDNA fragments of human DCP1A and human EXOSC5 were amplified from a 293T cDNA library by PCR, and cloned into the EcoRI/NotI sites of pcDNA3–RFP to produce pcDNA3–RFP–DCP1A and pcDNA3–RFP–EXOSC5.

Mice, Cells, and Viruses. C57BL/6 mice were purchased from CLEA Japan, Inc. *Irf3*$^{-/-}$*Irf7*$^{-/-}$ mice were kindly donated by T. Taniguchi (The University of Tokyo, Tokyo, Japan). The *Ddx58*$^{-/-}$*Ifih1*$^{-/-}$ mice have been described previously (45). The mice were maintained in our animal facility and treated in accordance with the guidelines of Osaka University. Primary MEFs were prepared from pregnant female mice on embryonic day 13.5, as described previously (4). To prepare bone marrow-derived dendritic cells, mouse bone marrow cells were cultured in the presence of 10 ng/mL GM-CSF (PeproTech) for 6 d, during which time the culture medium was replaced with medium containing GM-CSF every 2 d. The 293T cells have been described previously (46). Replication-competent MLV was produced by 293T cells transfected with pMLV-48. To induce infection, MLV was incubated with MEFs for 2 h in the presence of 10 μg/mL Polybrene (Millipore). VSV, IAV (A/Puerto Rico/8/34, H1N1 strain), and NDV have been described elsewhere (3, 4).

Quantitative RT-PCR. Total RNA was isolated using the ZR RNA MicroPrep kit (Zymo Research), according the manufacturer's instructions. Viral RNA was isolated from the culture supernatants using the ZR Viral RNA kit (Zymo Research), according the manufacturer's instructions. RT was performed using random primers and Verso reverse transcriptase (Thermo Scientific) according to the manufacturer's instructions. For quantitative PCR, the cDNA fragments were amplified from the RT products with Real-Time PCR Master Mix (Toyobo) according to the manufacturer's instructions. The fluorescence from the TaqMan probe for each cytokine was detected with a 7500 Real-Time PCR System (Applied Biosystems). To determine the relative induction of cytokine mRNAs, the level of mRNA expressed from each gene was normalized to the expression of 18S RNA. The copy number of the MLV genomic RNA was determined with the dsDNA copy number calculator program. The experiments were repeated at least three times, with reproducible results.

ELISAs. The levels of IFN-β and Cxcl10 in the culture supernatants were measured with ELISAs in accordance with the manufacturer's instructions. The experiments were repeated at least three times, with reproducible results.

Northern Blotting. Cytoplasmic RNA was extracted using the Cytoplasmic and Nuclear RNA Purification Kit (Norgen) according the manufacturer's instructions. The RNA obtained was separated electrophoretically, transferred to nylon membranes, and hybridized with the indicated probes. An RNA probe was designed to hybridize specifically to the Gag region from nucleotide 1291 to nucleotide 1472 of the MLV transcripts. The experiments were repeated at least three times, with reproducible results.

Immunoblotting. Immunoblotting was performed as described previously (47). The experiments were repeated at least three times, with reproducible results.

Immunostaining Assay. Cells cultured in microscopy chambers (ibidi) were fixed with 3% (wt/vol) paraformaldehyde and then processed for immunostaining as described previously (47). The samples were examined under an LSM 780 confocal laser scanning microscope (Carl Zeiss). The experiments were repeated at least three times, with reproducible results.

Detection of the MLV Transcripts with FISH. The cells were fixed with 4% paraformaldehyde. FISH was performed using the QuantiGene ViewRNA ISH Cell Assay kit (Veritas) according to the manufacturer's instructions. A Cy5-labeled FISH probe was designed to hybridize specifically to the Gag region from nucleotide 607 to nucleotide 1833 of the MLV transcripts. The samples were examined under an LSM780 confocal laser scanning microscope. The experiments were repeated at least three times, with reproducible results.

ACKNOWLEDGMENTS. We thank Drs. H. Fan, D. Trono, H. Miyoshi, and T. Taniguchi for providing invaluable materials and the members of the Laboratory of Host Defenses for their assistance. This work was supported by a Japan Society for the Promotion of Science Grant-in-Aid for Challenging Exploratory Research (to T. Saitoh); the Cabinet Office, Government of Japan, and the Japan Society for the Promotion of Science Funding Program for World-Leading Innovative Research and Development on Science and Technology "FIRST Program" (to S.A.); and National Institutes of Health Grant P01-AI070167 (to S.A.).

1. Kawai T, Akira S (2009) The roles of TLRs, RLRs and NLRs in pathogen recognition. *Int Immunol* 21(4):317–337.
2. Iwasaki A (2012) A virological view of innate immune recognition. *Annu Rev Microbiol* 66:177–196.
3. Yoneyama M, et al. (2004) The RNA helicase RIG-I has an essential function in double-stranded RNA-induced innate antiviral responses. *Nat Immunol* 5(7):730–737.
4. Kato H, et al. (2006) Differential roles of MDA5 and RIG-I helicases in the recognition of RNA viruses. *Nature* 441(7089):101–105.
5. Yoneyama M, et al. (1998) Direct triggering of the type I interferon system by virus infection: Activation of a transcription factor complex containing IRF-3 and CBP/p300. *EMBO J* 17(4):1087–1095.
6. Honda K, et al. (2005) IRF-7 is the master regulator of type-I interferon-dependent immune responses. *Nature* 434(7034):772–777.
7. Alexopoulou L, Holt AC, Medzhitov R, Flavell RA (2001) Recognition of double-stranded RNA and activation of NF-kappaB by Toll-like receptor 3. *Nature* 413(6857): 732–738.
8. Yamamoto M, et al. (2003) Role of adaptor TRIF in the MyD88-independent toll-like receptor signaling pathway. *Science* 301(5633):640–643.
9. Cella M, et al. (1999) Plasmacytoid monocytes migrate to inflamed lymph nodes and produce large amounts of type I interferon. *Nat Med* 5(8):919–923.
10. Diebold SS, Kaisho T, Hemmi H, Akira S, Reis e Sousa C (2004) Innate antiviral responses by means of TLR7-mediated recognition of single-stranded RNA. *Science* 303(5663):1529–1531.
11. Heil F, et al. (2004) Species-specific recognition of single-stranded RNA via toll-like receptor 7 and 8. *Science* 303(5663):1526–1529.
12. Kawai T, et al. (2004) Interferon-alpha induction through Toll-like receptors involves a direct interaction of IRF7 with MyD88 and TRAF6. *Nat Immunol* 5(10):1061–1068.
13. Honda K, et al. (2005) Spatiotemporal regulation of MyD88-IRF-7 signalling for robust type-I interferon induction. *Nature* 434(7036):1035–1040.
14. Ihle JN, Rein A, Mural R (1984) Immunological and virological mechanisms in retrovirus-induced murine leukemogenesis. *Advances in Viral Oncology*, ed Klein G (Raven Press, New York), pp 95–137.
15. Schiff RD, Oliff A (1986) The pathophysiology of murine retrovirus-induced leukemias. *Crit Rev Oncol Hematol* 5(3):257–323.
16. Kane M, et al. (2011) Innate immune sensing of retroviral infection via Toll-like receptor 7 occurs upon viral entry. *Immunity* 35(1):135–145.
17. Everitt AR, et al.; GenISIS Investigators; MOSAIC Investigators (2012) IFITM3 restricts the morbidity and mortality associated with influenza. *Nature* 484(7395):519–523.
18. Fensterl V, et al. (2012) Interferon-induced Ifit2/ISG54 protects mice from lethal VSV neuropathogenesis. *PLoS Pathog* 8(5):e1002712.
19. Goubau D, Deddouche S, Reis E Sousa C (2013) Cytosolic sensing of viruses. *Immunity* 38(5):855–869.
20. Gao G, Guo X, Goff SP (2002) Inhibition of retroviral RNA production by ZAP, a CCCH-type zinc finger protein. *Science* 297(5587):1703–1706.
21. Guo X, Carroll JW, Macdonald MR, Goff SP, Gao G (2004) The zinc finger antiviral protein directly binds to specific viral mRNAs through the CCCH zinc finger motifs. *J Virol* 78(23):12781–12787.
22. Guo X, Ma J, Sun J, Gao G (2007) The zinc-finger antiviral protein recruits the RNA processing exosome to degrade the target mRNA. *Proc Natl Acad Sci USA* 104(1): 151–156.
23. Chen G, Guo X, Lv F, Xu Y, Gao G (2008) p72 DEAD box RNA helicase is required for optimal function of the zinc-finger antiviral protein. *Proc Natl Acad Sci USA* 105(11): 4352–4357.
24. Ye P, Liu S, Zhu Y, Chen G, Gao G (2010) DEXH-Box protein DHX30 is required for optimal function of the zinc-finger antiviral protein. *Protein Cell* 1(10):956–964.
25. Wang X, Lv F, Gao G (2010) Mutagenesis analysis of the zinc-finger antiviral protein. *Retrovirology* 7:19.
26. Reineke LC, Lloyd RE (2013) Diversion of stress granules and P-bodies during viral infection. *Virology* 436(2):255–267.
27. Liu Q, Greimann JC, Lima CD (2006) Reconstitution, activities, and structure of the eukaryotic RNA exosome. *Cell* 127(6):1223–1237.
28. Hayakawa S, et al. (2011) ZAPS is a potent stimulator of signaling mediated by the RNA helicase RIG-I during antiviral responses. *Nat Immunol* 12(1):37–44.
29. Paprotka T, et al. (2011) Recombinant origin of the retrovirus XMRV. *Science* 333(6038):97–101.
30. Yamamoto N, Hinuma Y (1985) Viral aetiology of adult T-cell leukaemia. *J Gen Virol* 66(Pt 8):1641–1660.

31. Haseltine WA (1988) Replication and pathogenesis of the AIDS virus. *J Acquir Immune Defic Syndr* 1(3):217–240.
32. Zhu Y, et al. (2011) Zinc-finger antiviral protein inhibits HIV-1 infection by selectively targeting multiply spliced viral mRNAs for degradation. *Proc Natl Acad Sci USA* 108(38):15834–15839.
33. Müller S, et al. (2007) Inhibition of filovirus replication by the zinc finger antiviral protein. *J Virol* 81(5):2391–2400.
34. Bick MJ, et al. (2003) Expression of the zinc-finger antiviral protein inhibits alphavirus replication. *J Virol* 77(21):11555–11562.
35. Okeoma CM, Lovsin N, Peterlin BM, Ross SR (2007) APOBEC3 inhibits mouse mammary tumour virus replication in vivo. *Nature* 445(7130):927–930.
36. Santiago ML, et al. (2008) Apobec3 encodes Rfv3, a gene influencing neutralizing antibody control of retrovirus infection. *Science* 321(5894):1343–1346.
37. Yu P, et al. (2012) Nucleic acid-sensing Toll-like receptors are essential for the control of endogenous retrovirus viremia and ERV-induced tumors. *Immunity* 37(5):867–879.
38. Chen CY, et al. (2001) AU binding proteins recruit the exosome to degrade ARE-containing mRNAs. *Cell* 107(4):451–464.
39. Hurt JA, et al. (2009) A conserved CCCH-type zinc finger protein regulates mRNA nuclear adenylation and export. *J Cell Biol* 185(2):265–277.
40. Liang J, Song W, Tromp G, Kolattukudy PE, Fu M (2008) Genome-wide survey and expression profiling of CCCH-zinc finger family reveals a functional module in macrophage activation. *PLoS ONE* 3(8):e2880.
41. Lai WS, et al. (1999) Evidence that tristetraprolin binds to AU-rich elements and promotes the deadenylation and destabilization of tumor necrosis factor alpha mRNA. *Mol Cell Biol* 19(6):4311–4323.
42. Yu D, et al. (2007) Roquin represses autoimmunity by limiting inducible T-cell co-stimulator messenger RNA. *Nature* 450(7167):299–303.
43. Matsushita K, et al. (2009) Zc3h12a is an RNase essential for controlling immune responses by regulating mRNA decay. *Nature* 458(7242):1185–1190.
44. Bacheler L, Fan H (1981) Isolation of recombinant DNA clones carrying complete integrated proviruses of Moloney murine leukemia virus. *J Virol* 37(1):181–190.
45. Kato H, et al. (2008) Length-dependent recognition of double-stranded ribonucleic acids by retinoic acid-inducible gene-I and melanoma differentiation-associated gene 5. *J Exp Med* 205(7):1601–1610.
46. Saitoh Y, et al. (2008) Overexpressed NF-kappaB-inducing kinase contributes to the tumorigenesis of adult T-cell leukemia and Hodgkin Reed-Sternberg cells. *Blood* 111(10):5118–5129.
47. Saitoh T, et al. (2008) Loss of the autophagy protein Atg16L1 enhances endotoxin-induced IL-1beta production. *Nature* 456(7219):264–268.

HEPATOLOGY
Official Journal of the American Association for the Study of Liver Diseases

Human Blood Dendritic Cell Antigen 3 (BDCA3)$^+$ Dendritic Cells Are a Potent Producer of Interferon-λ in Response to Hepatitis C Virus

Sachiyo Yoshio,[1] Tatsuya Kanto,[1] Shoko Kuroda,[1] Tokuhiro Matsubara,[1] Koyo Higashitani,[1] Naruyasu Kakita,[1] Hisashi Ishida,[1] Naoki Hiramatsu,[1] Hiroaki Nagano,[2] Masaya Sugiyama,[3] Kazumoto Murata,[3] Takasuke Fukuhara,[4] Yoshiharu Matsuura,[4] Norio Hayashi,[5] Masashi Mizokami,[3] and Tetsuo Takehara[1]

The polymorphisms in the interleukin (*IL*)-*28B* (interferon-lambda [IFN]-λ3) gene are strongly associated with the efficacy of hepatitis C virus (HCV) clearance. Dendritic cells (DCs) sense HCV and produce IFNs, thereby playing some cooperative roles with HCV-infected hepatocytes in the induction of interferon-stimulated genes (ISGs). Blood dendritic cell antigen 3 (BDCA3)$^+$ DCs were discovered as a producer of IFN-λ upon Toll-like receptor 3 (TLR3) stimulation. We thus aimed to clarify the roles of BDCA3$^+$ DCs in anti-HCV innate immunity. Seventy healthy subjects and 20 patients with liver tumors were enrolled. BDCA3$^+$ DCs, in comparison with plasmacytoid DCs and myeloid DCs, were stimulated with TLR agonists, cell-cultured HCV (HCVcc), or Huh7.5.1 cells transfected with HCV/JFH-1. BDCA3$^+$ DCs were treated with anti-CD81 antibody, inhibitors of endosome acidification, TIR-domain-containing adapter-inducing interferon-β (TRIF)-specific inhibitor, or ultraviolet-irradiated HCVcc. The amounts of IL-29/IFN-λ1, IL-28A/IFN-λ2, and IL-28B were quantified by subtype-specific enzyme-linked immunosorbent assay (ELISA). The frequency of BDCA3$^+$ DCs in peripheral blood mononuclear cell (PBMC) was extremely low but higher in the liver. BDCA3$^+$ DCs recovered from PBMC or the liver released large amounts of IFN-λs, when stimulated with HCVcc or HCV-transfected Huh7.5.1. BDCA3$^+$ DCs were able to induce ISGs in the coexisting JFH-1-positive Huh7.5.1 cells. The treatments of BDCA3$^+$ DCs with anti-CD81 antibody, cloroquine, or bafilomycin A1 reduced HCVcc-induced IL-28B release, whereas BDCA3$^+$ DCs comparably produced IL-28B upon replication-defective HCVcc. The TRIF-specific inhibitor reduced IL-28B release from HCVcc-stimulated BDCA3$^+$ DCs. In response to HCVcc or JFH-1-Huh7.5.1, BDCA3$^+$ DCs in healthy subjects with IL-28B major (rs8099917, TT) released more IL-28B than those with IL-28B minor genotype (TG). *Conclusion*: Human BDCA3$^+$ DCs, having a tendency to accumulate in the liver, recognize HCV in a CD81-, endosome-, and TRIF-dependent manner and produce substantial amounts of IL-28B/IFN-λ3, the ability of which is superior in subjects with IL-28B major genotype. (HEPATOLOGY 2013;57:1705-1715)

Hepatitis C virus (HCV) infection is one of the most serious health problems in the world. More than 170 million people are chronically infected with HCV and are at high risk of developing liver cirrhosis and hepatocellular carcinoma. Genome-wide association studies have successfully identified the genetic polymorphisms (single nucleotide polymorphisms, SNPs) upstream of the promoter region of the

Abbreviations: Ab, antibody; HCV, hepatitis C virus; HCVcc, cell-cultured hepatitis C virus; HSV, herpes simplex virus; IHL, intrahepatic lymphocyte; INF-λ, interferon-lambda; IRF, interferon regulatory factor; ISGs, interferon-stimulated genes; JEV, Japanese encephalitis virus; Lin, lineage; mDC, myeloid DC; MOI, multiplicity of infection; PBMC, peripheral blood mononuclear cell; pDC, plasmacytoid DC; Poly IC, polyinosine-polycytidylic acid; RIG-I, retinoic acid-inducible gene-I; SNPs, single nucleotide polymorphisms; TLR, Toll-like receptor; TRIF, TIR-domain-containing adapter-inducing interferon-β.

From the [1]Department of Gastroenterology and Hepatology, Osaka University Graduate School of Medicine, Osaka, Japan; [2]Department of Surgery, Osaka University Graduate School of Medicine, Osaka, Japan; [3]Research Center for Hepatitis and Immunology, National Center for Global Health and Medicine, Ichikawa, Japan; [4]Department of Molecular Virology, Research Institute for Microbial Diseases, Osaka University, Osaka, Japan; [5]Kansai Rosai Hospital, Hyogo, Japan.

Received July 2, 2012; accepted November 13, 2012.

Supported in part by a Grant-In-Aid for Scientific Research from the Ministry of Education, Culture, Sports, Science, and Technology, Japan and a Grant-In-Aid from the Ministry of Health, Labor, and Welfare of Japan.

interleukin (IL)-28B / interferon-lambda 3 (IFN-λ3) gene, which are strongly associated with the efficacy of pegylated interferon-α (PEG-IFN-α) and ribavirin therapy or spontaneous HCV clearance.[1-4]

IFN-λs, or type III IFNs, comprise a family of highly homologous molecules consisting of IFN-λ1 (IL-29), IFN-λ2 (IL-28A), and IFN-λ3 (IL-28B). In clear contrast to type I IFNs, they are released from relatively restricted types of cells, such as hepatocytes, intestinal epithelial cells, or dendritic cells (DCs). Also, the cells that express heterodimeric IFN-λ receptors (IFN-λR1 and IL-10R2) are restricted to cells of epithelial origin, hepatocytes, or DCs.[5] Such limited profiles of cells expressing IFN-λs and their receptors define the biological uniqueness of IFN-λs. It has been shown that IFN-λs convey anti-HCV activity by inducing various interferon-stimulated genes (ISGs),[5] the profiles of which were overlapped but others were distinct from those induced by IFN-α/β. Some investigators showed that the expression of IL-28 in PBMC was higher in subjects with IL-28B major than those with minor; however, the levels of IL-28 transcripts in liver tissue were comparable regardless of IL-28B genotype.[2,6]

At the primary exposure to hosts, HCV maintains high replicative levels in the infected liver, resulting in the induction of IFNs and ISGs. In a case of successful HCV eradication, it is postulated that IFN-α/β and IFN-λ cooperatively induce antiviral ISGs in HCV-infected hepatocytes. It is of particular interest that, in primary human hepatocytes or chimpanzee liver, IFN-λs, but not type I IFNs, are primarily induced after HCV inoculation, the degree of which is closely correlated with the levels of ISGs.[7] These results suggest that hepatic IFN-λ could be a principal driver of ISG induction in response to HCV infection. Nevertheless, the possibility remains that DCs, as a prominent IFN producer in the liver, play significant roles in inducing hepatic ISGs and thereby suppressing HCV replication.

DCs, as immune sentinels, sense specific genomic and/or structural components of pathogens with various pattern recognition receptors and eventually release IFNs and inflammatory cytokines.[8] In general, DCs migrate to the organ where inflammation or cellular apoptosis occurs and alter their function in order to alleviate or exacerbate the disease conditions. Therefore, the phenotypes and/or capacity of liver DCs are deemed to be influenced in the inflamed liver. In humans, the existence of phenotypically and functionally distinct DC subsets has been reported: myeloid DC (mDC) and plasmacytoid DC (pDC).[9] Myeloid DCs predominantly produce IL-12 or tumor necrosis factor alpha (TNF-α) following proinflammatory stimuli, while pDCs release considerable amounts of type I IFNs upon virus infection.[9] The other type of mDCs, mDC2 or BDCA3$^+$(CD141) DCs, have been drawing much attention recently, since human BDCA3$^+$ DCs are reported to be a counterpart of murine CD8a$^+$ DCs.[10] Of particular interest is the report that BDCA3$^+$ DCs have a potent capacity of releasing IFN-λ in response to Toll-like receptor 3 (TLR3) agonist.[11] However, it is still largely unknown whether human BDCA3$^+$ DCs are able to respond to HCV.

Taking these reports into consideration, we hypothesized that human BDCA3$^+$ DCs, as a producer of IFN-λs, have crucial roles in anti-HCV innate immunity. We thus tried to clarify the potential of BDCA3$^+$ DCs in producing type III IFNs by using cell-cultured HCV (HCVcc) or hepatoma cells harboring HCV as stimuli. Our findings show that BDCA3$^+$ DCs are quite a unique DC subset, characterized by a potent and specialized ability to secrete IFN-λs in response to HCV. The ability of BDCA3$^+$ DCs to release IL-28B upon HCV is superior in subjects with IL-28B major (rs8099917, TT) to those with minor (TG or GG) genotype, suggesting that BDCA3$^+$ DCs are one of the key players in IFN-λ-mediated innate immunity.

Patients and Methods

Subjects. This study enrolled 70 healthy volunteers (male/female: 61/9) (age: mean ± standard deviation [SD], 37.3 ± 7.8 years) and 20 patients who underwent surgical resection of liver tumors at Osaka University Hospital (Supporting Table 1). The study was approved by the Ethical Committee of Osaka University Graduate School of Medicine. Written informed consent was obtained from all of them. All healthy volunteers were negative for HCV, hepatitis B virus (HBV), and human immunodeficiency virus (HIV) and had no apparent history of liver, autoimmune, or malignant diseases.

Address reprint requests to: Tatsuya Kanto, M.D., Ph.D., Department of Gastroenterology and Hepatology, Osaka University Graduate School of Medicine, 2-2 Yamadaoka, Suita, 565-0871 Japan. E-mail: kantot@gh.med.osaka-u.ac.jp; fax: +81-6-6879-3629.

View this article online at wileyonlinelibrary.com.
DOI 10.1002/hep.26182
Potential conflict of interest: Nothing to report.
Additional Supporting Information may be found in the online version of this article.

Reagents. The specifications of all antibodies used for FACS or cell sorting TLR-specific synthetic agonists, pharmacological reagents, and inhibitory peptides are listed in the Supporting Materials.

Separation of DCs from PBMC or Intrahepatic Lymphocytes. We collected 400 mL of blood from each healthy volunteer and processed them for PBMCs. Noncancerous liver tissues were obtained from patients who underwent resection of liver tumors (Supporting Table 1). For the collection of intrahepatic lymphocytes (IHLs), liver tissues were washed thoroughly with phosphate-buffered saline to remove the peripheral blood adhering to the tissue and ground gently. After Lin-negative ($CD3^-$, $CD14^-$, $CD19^-$, and $CD56^-$) cells were obtained by the MACS system, each DC subset with the defined phenotype was sorted separately under FACS Aria (BD). The purity was more than 98%, as assessed by FACS Canto II (BD). Sorted DCs were cultured at 2.5×10^4/well on 96-well culture plates.

Immunofluorescence Staining of Human Liver Tissue. Tissue specimens were obtained from surgical resections of noncancerous liver from the patients as described above. Briefly, the 5-mm sections were incubated with the following antibodies: mouse biotinylated antihuman BDCA3 antibody (Miltenyi-Biotec), and mouse antihuman CLEC9A antibody (Biolegend) and subsequently with secondary goat antirabbit Alexa Fluor488 or goat antimouse Alexa Fluor594 (Invitrogen, Molecular Probes) antibodies. Cell nuclei were counterstained with Dapi-Fluoromount-GTM (Southern Biotech, Birmingham, AL). The stained tissues were analyzed by fluorescence microscopy (Model BZ-9000; Keyence, Osaka, Japan).

Cells and Viruses. The *in vitro* transcribed RNA of the JFH-1 strain of HCV was introduced into FT3-7 cells[12] or Huh7.5.1 cells. The stocks of HCVcc were generated by concentration of the medium from JFH-1-infected FT3-7 cells. The virus titers were determined by focus forming assay.[13] The control medium was generated by concentration of the medium from HCV-uninfected FT3-7 cells. Infectious JEVs were generated from the expression plasmid (pMWJEATG1) as reported.[14] HSV (KOS) was a generous gift from Dr. K. Ueda (Osaka University). Huh7.5.1 cells transduced with HCV JFH-1 strain was used for the coculture with DCs. The transcripts of ISGs in Huh7.5.1 were examined by reverse-transcription polymerase chain reaction (RT-PCR) methods using gene-specific primers and probes (Applied Biosystems, Foster City, CA).

Secretion Assays. IL-28B/IFN-λ3 was quantified by a newly developed chemiluminescence enzyme immunoassay (CLEIA) system.[15] IL-29/IFN-λ1, IL-28A/IFN-λ2, and IFN-β were assayed by commercially available enzyme-linked immunosorbent assay (ELISA) kits (eBioscience, R&D, and PBL, respectively). IFN-α was measured by cytometric beads array kits (BD) according to the manufacturer's instructions.

Statistical Analysis. The differences between two groups were assessed by the Mann-Whitney nonparametric *U* test. Multiple comparisons between more than two groups were analyzed by the Kruskal-Wallis nonparametric test. Paired *t* tests were used to compare differences in paired samples. All the analyses were performed using GraphPad Prism software (San Diego, CA).

Results

Human BDCA3$^+$ DCs Are Phenotypically Distinct from pDCs and mDCs. We defined BDCA3$^+$ DCs as $Lin^-HLA\text{-}DR^+BDCA3^{high+}$ cells (Fig. 1A, left, middle), and pDCs and mDCs by the patterns of CD11c and CD123 expressions (Fig. 1A, right). The level of CD86 on pDCs or mDCs is comparatively higher than those on BDCA3$^+$ DCs (Fig. 1B). The expression of CD81 is higher on BDCA3$^+$ DCs than on pDCs and mDCs (Fig. 1B, Supporting Fig. S1). CLEC9A, a member of C-type lectin, is expressed specifically on BDCA3$^+$ DCs as reported elsewhere,[16] but not on pDCs and mDCs (Fig. 1B).

Liver BDCA3$^+$ DCs Are More Mature than the Counterparts in the Periphery. BDCA3$^+$ DCs in infiltrated hepatic lymphocytes (IHLs) are all positive for CLEC9A, but liver pDCs or mDCs are not (data not shown). The levels of CD40, CD80, CD83, and CD86 on liver BDCA3$^+$ DCs are higher than those on the peripheral counterparts, suggesting that BDCA3$^+$ DCs are more mature in the liver compared to those in the periphery (Fig. 1C).

In order to confirm that BDCA3$^+$ DCs are localized in the liver, we stained the cells with immunofluorescence antibodies (Abs) in noncancerous liver tissues. Liver BDCA3$^+$ DCs were defined as BDCA3$^+$ CLEC9A$^+$ cells (Fig. 1D). Most of the cells were found near the vascular compartment or in sinusoid or the space of Disse of the liver tissue.

BDCA3$^+$ DCs Are Scarce in PBMCs but More Abundant in the Liver. The percentages of BDCA3$^+$ DCs in PBMCs were much lower than those of the other DC subsets (BDCA3$^+$ DCs, pDCs and mDCs, mean $\pm$ SD [%], 0.054 ± 0.044, 0.27 ± 0.21 and 1.30 ± 0.65) (Fig. 2A). The percentages of BDCA3$^+$ DCs in IHLs were lower than those of the others (BDCA3$^+$ DCs, pDCs, and mDCs, mean $\pm$ SD [%],

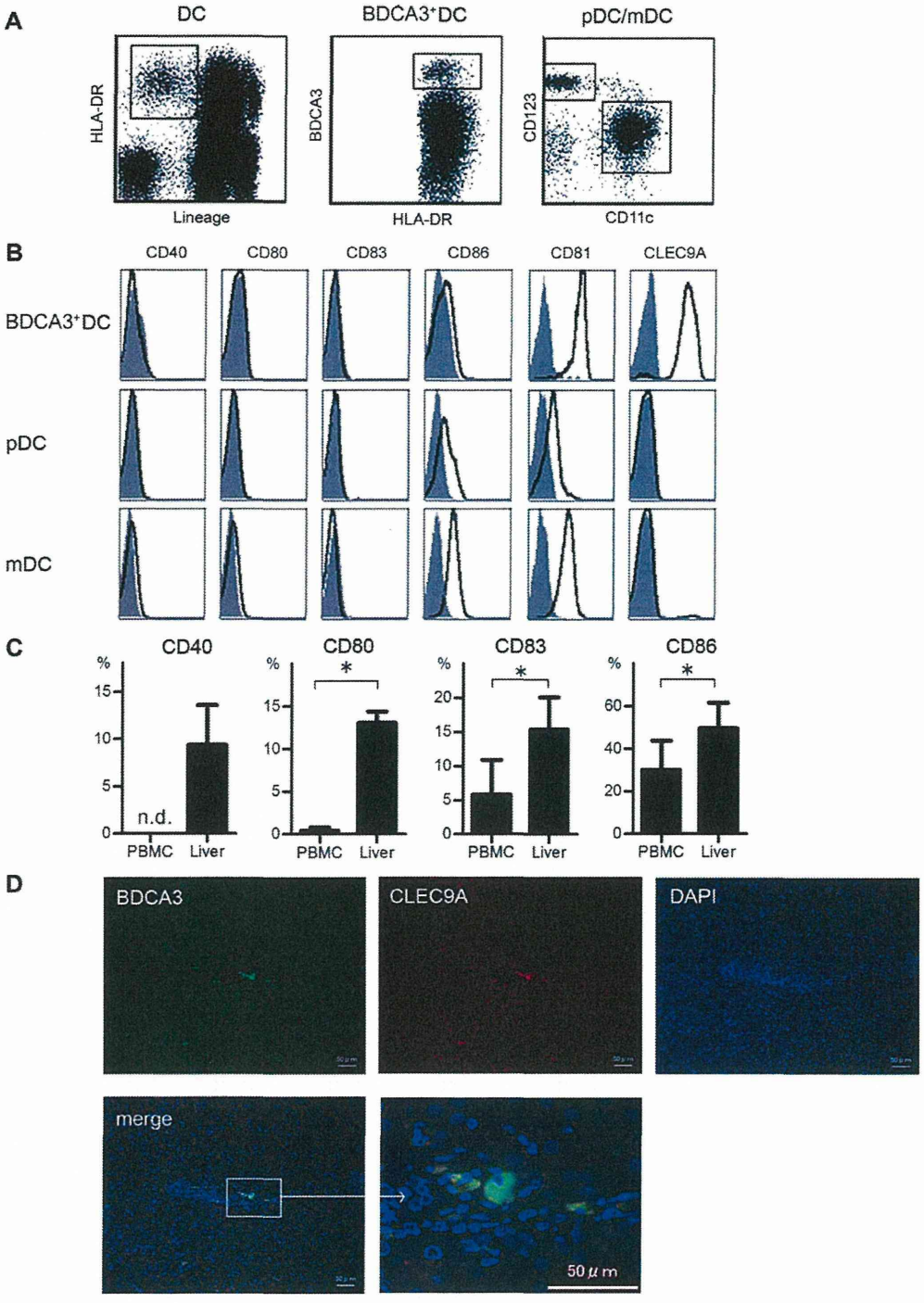

Fig. 1. Identification and phenotypic analyses of peripheral blood and intrahepatic BDCA3$^+$ DCs. (A) We defined BDCA3$^+$ DCs as Lineage$^-$HLA-DR$^+$BDCA3^{high+} cells (middle), pDCs as Lineage$^-$HLA-DR$^+$CD11c$^-$CD123^{high+} cells, and mDCs as Lineage$^-$HLA-DR$^+$CD11c$^+$CD123^{low+} cells (right). (B) The expressions of CD40, CD80, CD83, CD86, CD81, and CLEC9A on each DC subset in peripheral blood are shown. Representative results of five donors are shown in the histograms. Filled gray histograms depict data with isotype Abs, and open black ones are those with specific Abs. (C) The expressions of costimulatory molecules on BDCA3$^+$ DCs were compared between in PBMCs and in the liver. The results are shown as the percentage of positive cells. Results are the mean ± SEM from four independent experiments. *$P < 0.05$ by paired t test. (D) The staining for BDCA3 (green), CLEC9A (red) identifies BDCA3$^+$ DCs (merge, BDCA3$^+$CLEC9A$^+$) in human liver tissues. Representative results of the noncancerous liver samples are shown. BDCA, blood dendritic cell antigen; pDC, plasmacytoid DC; mDC, myeloid DC; CLEC9A, C-type lectin 9A.

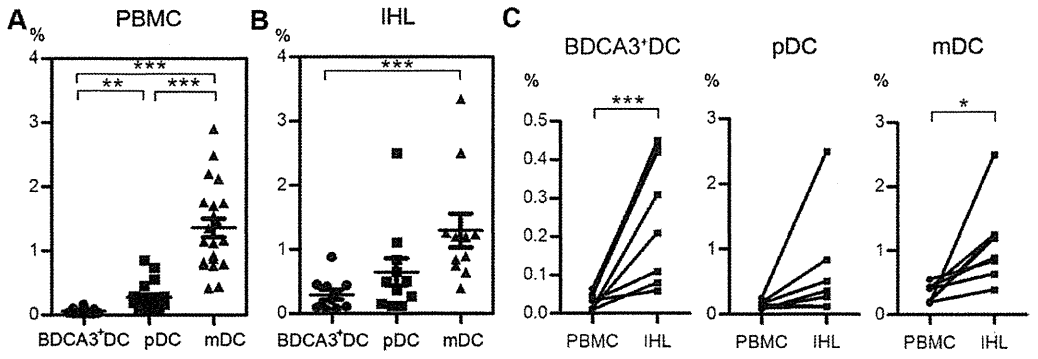

Fig. 2. Analysis of frequency of DC subsets in the peripheral blood and in the liver. Frequencies of BDCA3$^+$ DCs, pDCs, and mDCs in PBMCs (21 healthy subjects) (A) or in the intrahepatic lymphocytes (IHLs) (11 patients who had undergone surgical resection of tumors) (B) are shown. Horizontal bars depict the mean ± SD. $^{**}P < 0.005$; $^{***}P < 0.0005$ by Kruskal-Wallis test. (C) The paired comparisons of the frequencies of DC subsets between in PBMCs and in IHLs. the results of eight patients whose PBMCs and IHLs were obtained simultaneously are shown. $^{*}P < 0.05$; $^{***}P < 0.0005$ by paired *t* test. IHLs, intrahepatic lymphocytes; pDC and mDC, see Fig. 1.

0.29 ± 0.25, 0.65 ± 0.69 and 1.2 ± 0.94) (Fig. 2B). The percentages of BDCA3$^+$ DCs in the IHLs were significantly higher than those in PBMCs from relevant donors (Fig. 2C). Such relative abundance of BDCA3$^+$ DCs in the liver over that in the periphery was observed regardless of the etiology of the liver disease (Supporting Table 1).

BDCA3$^+$ DCs Produce a Large Amount of IFN-λs upon Poly IC Stimulation. We compared DC subsets for their abilities to produce IL-29/IFN-λ1, IL-28A/IFN-λ2, IL-28B/IFN-λ3, IFN-β, and IFN-α in response to TLR agonists. Approximately 4.0 × 10^4 of BDCA3$^+$ DCs were recoverable from 400 mL of donated blood from healthy volunteers. We fixed the number of DCs at 2.5 × 10^4 cells/100 mL for comparison in the following experiments.

BDCA3$^+$ DCs have been reported to express mRNA for TLR1, 2, 3, 6, 8, and 10.[17] First, we quantified IL-28B/IFN-λ3 as a representative for IFN-λs after stimulation of BDCA3$^+$ DCs with relevant TLR agonists. We confirmed that BDCA3$^+$ DCs released IL-28B robustly in response to TLR3 agonist/poly IC but not to other TLR agonists (Fig. S2). In contrast, pDCs produced IL-28B in response to TLR9 agonist/CpG but much lesser to other agonists (Fig. S2). Next, we compared the capabilities of DCs inducing IFN-λs and IFN-β genes in response to relevant TLR agonists. BDCA3$^+$ DCs expressed extremely high levels of IL-29, IL-28A, and IL-28B transcripts compared to other DCs, whereas pDCs induced a higher level of IFN-β than other DCs (Fig. S3A).

Similar results were obtained with the protein levels of IFN-λs, IFN-β, and IFN-α released from DC subsets stimulated with TLR agonists. BDCA3$^+$ DCs produce significantly higher levels of IL-29, IL-28B, and IL-28A than the other DC subsets. In clear contrast, pDCs release a significantly larger amount of IFN-β and IFN-α than BDCA3$^+$ DCs or mDCs (Fig. 3A, Fig. S3B). As for the relationship among the quantity of IFN-λ subtypes from poly IC-stimulated BDCA3$^+$ DCs, the levels of IL-29/IFN-λ1 and IL-28B/IFN-λ3 were positively correlated ($R^2 = 0.76$, $P < 0.05$), and those of IL-28A/IFN-λ2 and IL-28B/IFN-λ3 were positively correlated as well ($R^2 = 0.84$, $P < 0.0005$), respectively (Fig. S3C). These results show that the transcription and translation machineries of IFN-λs may be overlapped among IFN-λ subtypes in BDCA3$^+$ DCs upon poly IC stimulation.

Liver BDCA3$^+$ DCs sorted from IHLs possess the ability to produce IL-28B in response to poly IC (Fig. 3B), showing that they are comparably functional. In response to poly IC, BDCA3$^+$ DCs were capable of producing inflammatory cytokines as well, such as TNF-α, IL-6, and IL-12p70 (Fig. S4A). By using Huh7 cells harboring HCV subgenomic replicons (HCV-N, genotype 1b), we confirmed that the supernatants from poly IC-stimulated BDCA3$^+$ DCs suppressed HCV replication in an IL-28B concentration-dependent manner (Fig. S4B). Therefore, poly IC-stimulated BDCA3$^+$ DCs are capable of producing biologically active substances suppressing HCV replication, some part of which may be mediated by IFN-λs.

BDCA3$^+$ DCs Produce IL-28B upon HCVcc or HCV/JFH-1-Transfected Huh7.5.1 Cells. We stimulated freshly isolated BDCA3$^+$ DCs, pDCs and mDCs with infectious viruses, such as HCVcc, Japanese encephalitis virus (JEV), and herpes simplex virus (HSV). In preliminary experiments, we confirmed that HCVcc stimulated BDCA3$^+$ DCs to release IL-28B in a dose-dependent manner (Fig. S5). BDCA3$^+$ DCs

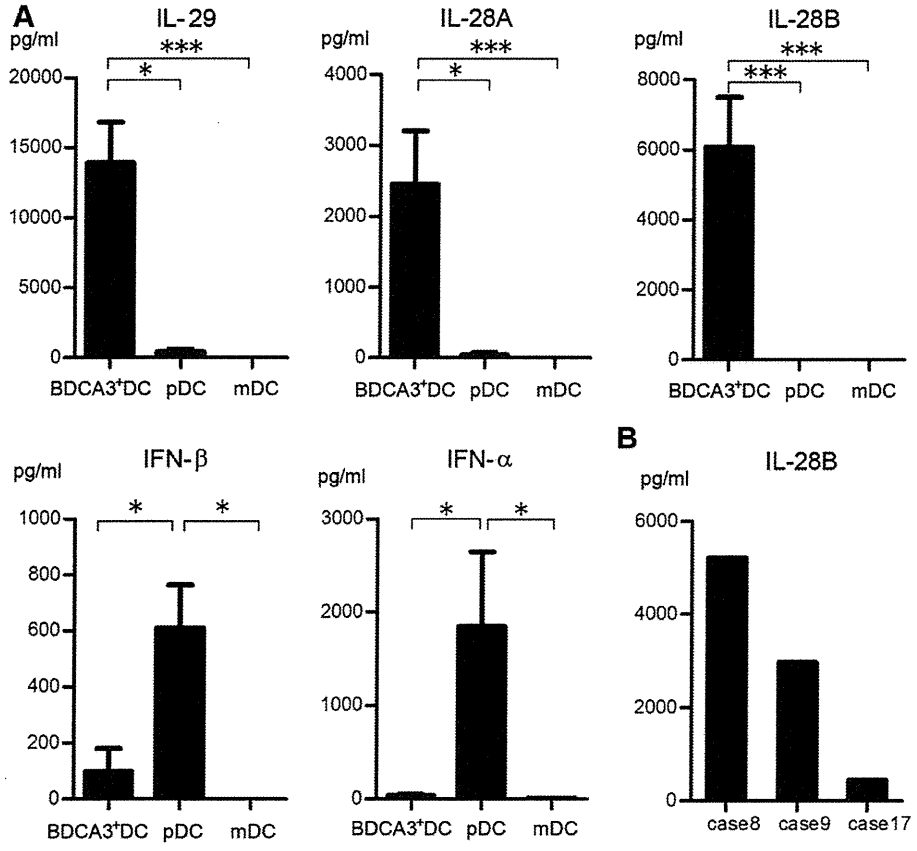

Fig. 3. BDCA3$^+$ DCs recovered from peripheral blood or intrahepatic lymphocytes produce large amounts of IL-29/IFN-λ1, IL-28A/IFN-λ2, and IL-28B/IFN-λ3 in response to poly IC. (A) BDCA3$^+$ DCs and mDCs were cultured at 2.5 $\times$ 10^4 cells with 25 mg/mL poly IC, and pDCs were with 5 mM CPG for 24 hours. The supernatants were examined for IL-29, IL-28A, IL-28B, IFN-β and IFN-α. Results are shown as mean $\pm$ SEM from 15 experiments. *P < 0.05; ***P < 0.0005 by Kruskal-Wallis test. (B) For the IL-28B production, BDCA3$^+$ DCs in intrahepatic lymphocytes were cultured at 2.5 $\times$ 10^4 cells with 25 mg/mL poly IC for 24 hours. The samples of cases 8 and 9 were obtained from patients with non-B, non-C liver disease and that of case 17 was from an HCV-infected patient (Supporting Table 1).

produced a large amount of IL-28B upon exposure to HCVcc and released a lower amount of IFN-α upon HCVcc or HSV (Fig. 4A). In contrast, pDCs produced a large amount of IFN-α in response to HCVcc and HSV and a much lower level of IL-28B upon HCVcc (Fig. S6). In mDCs, IL-28B and IFN-α were not detectable with any of these viruses (data not shown).

BDCA3$^+$ DCs produced significantly higher levels of IL-28B than the other DCs upon HCVcc stimulation (Fig. 4B). By contrast, HCVcc-stimulated pDCs released significantly larger amounts of IFN-β and IFN-α than the other subsets (Fig. 4B). Liver BDCA3$^+$ DCs were capable of producing IL-28B in response to HCVcc (Fig. 4C). These results show that, upon HCVcc stimulation, BDCA3$^+$ DCs produce more IFN-λs and pDCs release more IFN-β and IFN-α than the other DC subsets, respectively. Taking a clinical impact of IL-28B genotypes on HCV eradication into consideration, we focused on IL-28B/IFN-λ3 as a representative for IFN-λs in the following experiments.

In a coculture with JFH-1-infected Huh7.5.1 cells, BDCA3$^+$ DCs profoundly released IL-29, IL-28A, and IL-28B (Fig. 4D, the results of IL-29 and IL-28A, not shown), whereas BDCA3$^+$ DCs failed to respond to Huh7.5.1 cells lacking HCV/JFH-1, showing that IL-28B production from BDCA3$^+$ DCs is dependent on HCV genome (Fig. 4D). In the absence of BDCA3$^+$ DCs, IL-28B is undetectable in the supernatant from JFH-1-infected Huh7.5.1 cells, demonstrating that BDCA3$^+$ DCs, not HCV-replicating Huh7.5.1 cells, produce detectable amount of IL-28B (Fig. 4D). In the coculture, BDCA3$^+$ DCs comparably released IL-28B either in the presence or the absence of transwells, suggesting that cell-to-cell contact between DCs and Huh7.5.1 cells is dispensable for IL-28B response (Fig. 4E). In parallel with the quantity of IL-28B in the coculture, ISG15 was significantly induced only in JFH-1-infected Huh7.5.1 cells cocultured with BDCA3$^+$ DCs (Fig. 4F). A strong induction was observed with other ISGs in JFH-1-infected Huh7.5.1 in the presence of BDCA3$^+$ DCs, such as IFIT1, MxA, RSD2, IP-10, and USP18 (Fig. S7). The results clearly show that BDCA3$^+$ DCs are capable of producing large amounts of IFN-λs in response to cellular or cell-free HCV, thereby inducing various ISGs in bystander liver cells.

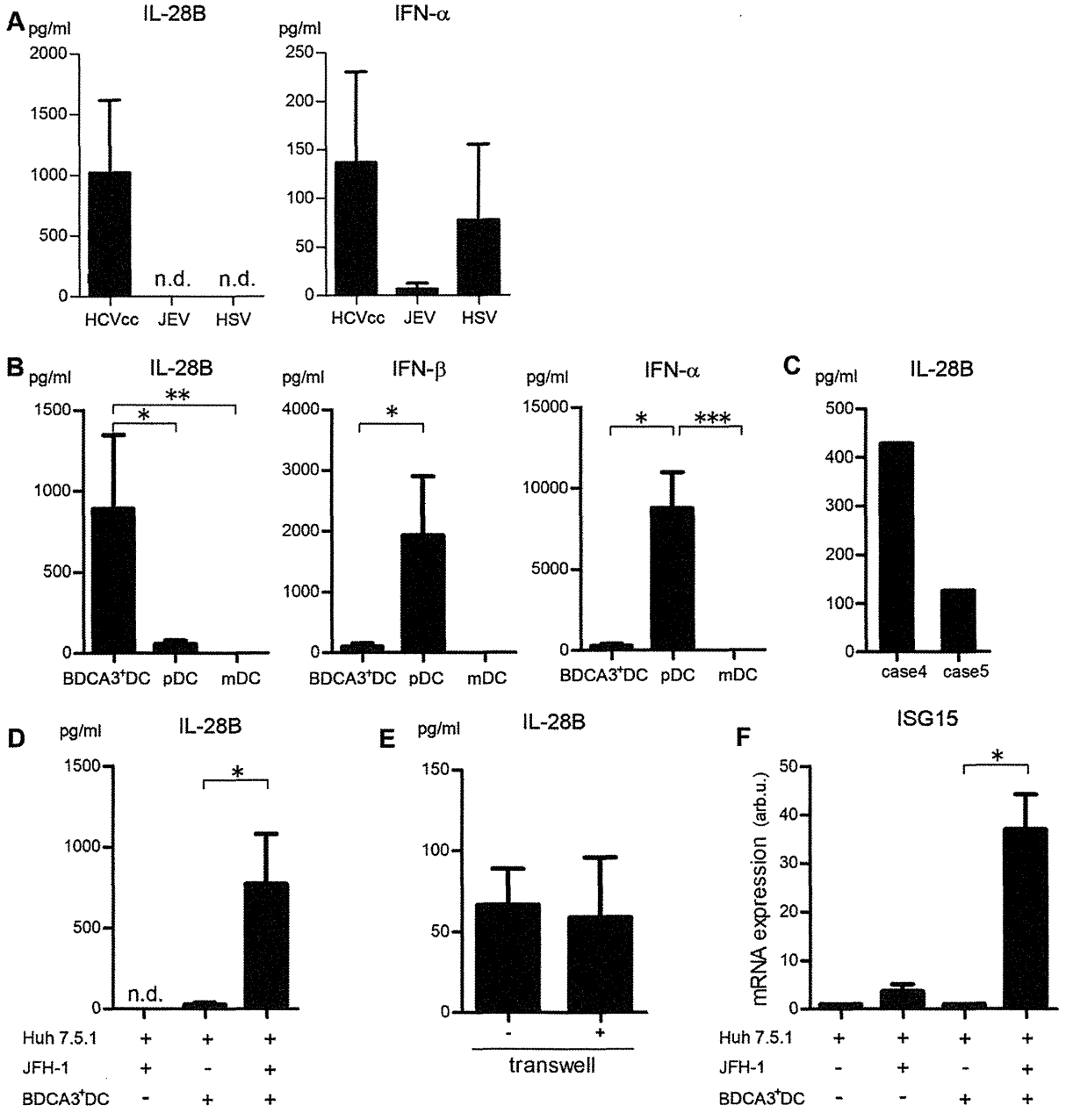

Fig. 4. BDCA3$^+$ DCs produce IL-29, IL-28A, and IL-28B upon cell-cultured HCV or HCV/JFH-1-transfected Huh7.5.1 cells, thereby inducing ISG. (A) BDCA3$^+$ DCs were cultured at 2.5 $\times$ 10^4 cells for 24 hours with HCVcc, JEV, or HSV at a multiplicity of infection (MOI) of 10. Results are shown as mean $\pm$ SEM from six experiments. n.d.; not detected. (B) BDCA3$^+$ DCs, pDCs, and mDCs were cultured at 2.5 $\times$ 10^4 cells for 24 hours with HCVcc at an MOI of 10. The results are shown as mean $\pm$ SEM from 11 experiments. *$P < 0.05$; **$P < 0.0005$; ***$P < 0.0005$ by Kruskal-Wallis test. (C) BDCA3$^+$ DCs recovered from intrahepatic lymphocytes were cultured at 2.5 $\times$ 10^4 cells for 24 hours with HCVcc at an MOI of 10. Both of the samples (cases 4 and 5) were obtained from patients with non-B, non-C liver disease. (D,E) BDCA3$^+$ DCs were cocultured at 2.5 $\times$ 10^4 cells with JFH-1-transfected (MOI = 2) or -untransfected Huh7.5.1 cells for 24 hours. The supernatants of JFH-1-transfected Huh7.5.1.cells without BDCA3$^+$ DCs were also examined. In some experiments of the coculture with JFH-1-transfected Huh7.5.1 cells and BDCA3$^+$ DCs, transwells were inserted into the wells (E). Results are shown as mean $\pm$ SEM from five experiments. *$P < 0.05$ by paired t test. (F) BDCA3$^+$ DCs were cocultured at 2.5 $\times$ 10^4 cells with JFH-1-transfected Huh7.5.1 cells. (MOI = 2) or -untransfected Huh7.5.1 cells for 24 hours. The Huh7.5.1.cells were harvested and subjected to real-time RT-PCR analyses for ISG15 expression. The results are shown as mean $\pm$ SEM from five experiments. *$P < 0.05$ by paired t test. HCVcc, cell-cultured HCV; JEV, Japanese encephalitis virus; HSV, herpes simplex virus.